arXiv:1610.06814v1 [math.NA] 21 Oct 2016

A CONVERGENT TIME-SPACE ADAPTIVE DG(S) FINITE ELEMENT METHOD FOR PARABOLIC PROBLEMS MOTIVATED BY EQUAL ERROR DISTRIBUTION

FERNANDO D. GASPOZ, CHRISTIAN KREUZER, KUNIBERT G. SIEBERT, AND DANIEL A. ZIEGLER

Abstract. We shall develop a fully discrete space-time adaptive method for linear parabolic problems based on new reliable and efficient a posteriori analysis for higher order dG(s) finite element discretisations. The adaptive strategy is motivated by the principle of equally distributing the a posteriori indicators in time and the convergence of the method is guaranteed by the uniform energy estimate from [KMSS12] under minimal assumptions on the regularity of the data.

1. Introduction

Let Ω be a bounded polyhedral domain in $\mathbb{R}^d$, $d \in \mathbb{N}$. We consider the linear parabolic partial differential equation

$$\begin{aligned} \partial_t u + \mathcal{L}u &= f && \text{in } \Omega \times (0,T) \\ u &= 0 && \text{on } \partial\Omega \times (0,T) \\ u(\cdot,0) &= u_0 && \text{in } \Omega. \end{aligned} \tag{1.1}$$

Hereafter, $\mathcal{L}u = -\operatorname{div} \mathbf{A}\nabla u + cu$ is a second order elliptic operator with respect to space and $\partial_t u = \frac{\partial u}{\partial t}$ denotes the partial derivative with respect to time. In the simplest setting $\mathcal{L} = -\Delta$, whence (1.1) is the heat equation. Precise assumptions on data are provided in Section 2.1.

The objective of this paper is the design and a detailed convergence analysis of an efficient adaptive finite element method for solving (1.1) numerically. To this end, we resort to adaptive finite elements in space combined with a discontinuous Galerkin dG(s) time-stepping scheme in Section 2.2. The conforming finite element spaces are continuous piecewise polynomials of fixed degree over a simplicial triangulation of the domain Ω. In each single time-step, we reduce or enlarge the local time-step size and refine and coarsen the underlying triangulation.

The adaptive decisions are based on a posteriori error indicators. Numerous such estimators for various error notions are available in the literature. Error bounds in $L^\infty(L^2)$ can e.g. be found in [EJ91] or [LM06], where the latter result is based on the elliptic reconstruction technique, which was introduced in [MN03] in the semi-discrete context. The $L^2(H^1)$ respectively $L^2(H^1) \cap H^1(H^{-1})$ error bounds in [Pic98, Ver03] are based on energy techniques and have been used with a dG(0) time-stepping scheme in the adaptive methods and convergence analysis presented in [CF04, KMSS12]. For our purpose, we generalise the residual based estimator [Ver03] to higher order dG(s) schemes in Section 3. The estimator is build from five indicators: an indicator for the initial error, indicators for the temporal and spatial errors, a coarsening error indicator, and an indicator controlling the so-called consistency error. It is important to notice that besides the first indicator

Date: October 24, 2016.

2000 *Mathematics Subject Classification.* Primary 65N30, 65N12, 65N50, 65N15.

Key words and phrases. Adaptive finite elements, parabolic problems, convergence.

all other indicators accumulate in L^2 in time. The adaptation of the time-step-size uses informations of the indicators for the temporal error and the consistency error. The adaptation of the spatial triangulation is based on refinement by bisection using information from the indicators for the spatial error and for the coarsening error. Very recently an independently developed guaranteed a posteriori estimator for higher order dG(s) schemes is provided in [ESV] using equilibrated flux based bounds for the spatial error.

By now the convergence and optimality of adaptive methods for stationary inf-sup stable respectively coercive problems is well-established [BDD04, CKNS08, CF04, DKS16, Dör96, DK08, KS11, MSV08, MN05, MNS00, MNS02, Sie11, Ste07]; compare also with the overview article [NSV09]. The essential design principle motivating the adaptive strategies in most of the above methods is the equal distribution of the error. The importance of this principle is highlighted by the near characterisations of nonlinear approximation classes with the help of a thresholding algorithm in [BDDP02, GM14].

In contrast to the situation for above mentioned problems, the convergence analysis of adaptive approximation of time-dependent problems is still in its infancy. In [SS09] optimal computational complexity of an adaptive wavelet method for parabolic problems is proved using a symmetric and coercive discretisation based on a least squares formulation. To our best knowledge, there exist only two results [CF04, KMSS12] concerned with a rigorous convergence analysis of time-space adaptive finite element methods. In [CF04], it is proved for the dG(0) time-stepping scheme, that each single time-step terminates and that the error of the computed approximation is below a prescribed tolerance when the final time is reached. This, however, is not guaranteed and thus theoretically the adaptively generated sequence of time instances $\{t_n\}_{n\geqslant 0}$ may not be finite and such that $t_n \to t_\star < T$ as $n \to \infty$. This drawback has been overcome in [KMSS12] with the help of an a priori computed minimal time-step size in terms of the right-hand side f and the discrete initial value U_0. However, neither design of the two methods heeds the principle of equally distributing the error. Let us shed some light on this fact with the help of the initial value problem

$$\partial_t u + u = f \quad \text{in } (0,T) \qquad \text{and} \qquad u(0) = u_0.$$

Let $0 = t_0 < t_1 < \ldots < t_N = T$ be some partition of $(0,T)$. Using the dG(0) time-stepping scheme we obtain $\{U_n\}_{n=0}^N$, such that

$$\frac{U_n - U_{n-1}}{\tau_n} + U_n = f_n := \frac{1}{\tau_n}\int_{t_{n-1}}^{t_n} f \,\mathrm{d}t, \quad n = 1, \ldots, N, \qquad U_0 = u_0,$$

where $\tau_n = t_n - t_{n-1}$. Let $\mathcal{U}$ be the piecewise affine interpolation $\mathcal{U}$ of the nodal values $\{U_n\}_{n=0}^N$. Then we have with Young's inequality, that

$$\begin{aligned}\int_0^T \frac{1}{2}\partial_t|u-\mathcal{U}|^2 + |u-\mathcal{U}|^2 \,\mathrm{d}t &= \sum_{n=1}^N \int_{t_{n-1}}^{t_n} (f-f_n)(u-\mathcal{U}) + (U_n - \mathfrak{u})(u-\mathcal{U})\,\mathrm{d}t \\ &\leqslant \sum_{n=1}^N \int_{t_{n-1}}^{t_n} |f-f_n|^2 + |U_n - \mathcal{U}|^2 + \frac{1}{2}|u-\mathcal{U}|^2 \,\mathrm{d}t.\end{aligned}$$

A simple computation reveals $\int_{t_{n-1}}^{t_n} |U_n - \mathcal{U}|^2 \,\mathrm{d}t = \frac{1}{3}\tau_n |U_n - U_{n-1}|^2$. This term and $\int_{t_{n-1}}^{t_n} |f - f_n|^2 \,\mathrm{d}t$ are the so-called time and consistency a posteriori indicators. In order to illustrate the basic differences in the design of the adaptive schemes, we shall concentrate on the time indicator. In [CF04, KMSS12] the partition is

constructed such that

$$|U_n - U_{n-1}|^2 \leqslant \frac{\texttt{TOL}^2}{T}, \quad \text{which implies} \quad \sum_{n=1}^{N} \tau_n |U_n - U_{n-1}|^2 \leqslant \sum_{n=1}^{N} \tau_n \frac{\texttt{TOL}^2}{T} = \texttt{TOL}^2,$$

i.e. the accumulated indicator is below the prescribed tolerance TOL. We call this the L^∞-strategy and remark that it does not aim at equally distributing the local indicators. In contrast to this, we shall use the L^2-strategy

$$\tau_n |U_n - U_{n-1}|^2 \leqslant \texttt{tol}^2.$$

Thanks to the uniform energy bound

$$\sum_{n=1}^{N} |U_n - U_{n-1}|^2 \leqslant \int_0^T |f|^2 \,\mathrm{d}t + |U_0|^2 \tag{1.2}$$

(see Corollary 11 below) we conclude then, that

$$\begin{aligned}\sum_{n=1}^{N} \tau_n |U_n - U_{n-1}|^2 &= \sum_{\tau_n \leqslant \delta}^{N} \tau_n |U_n - U_{n-1}|^2 + \sum_{\tau_n > \delta}^{N} \tau_n |U_n - U_{n-1}|^2 \\ &\leqslant \delta \Big(\int_0^T |f|^2 \,\mathrm{d}t + |U_0|^2 \Big) + \frac{T}{\delta} \texttt{tol}^2 = \left(\frac{T}{\int_0^T |f|^2 \,\mathrm{d}t + |U_0|^2} \right)^{\frac{1}{2}} \texttt{tol}\end{aligned}$$

where $\delta = (T/(\int_0^T |f|^2 \,\mathrm{d}t + |U_0|^2))^{1/2}$. Taking $\texttt{tol} = \texttt{TOL}^2/\delta$ guarantees that the error is below the prescribed tolerance TOL.

These arguments directly generalise to semi-discretisations of (1.1) in time. In the case of a full space-time discretisation of (1.1) additional indicators are involved, for which a control similar to (1.2) is not available. We therefore enforce that these indicators are bounded by the time or the consistency indicator. If these indicators are equally distributed in time, then this results also in an equal distribution of the other indicators. Otherwise, we shall use the L^∞-strategy from [CF04, KMSS12] as a backup strategy. The detailed algorithm TAFEM for (1.1) is presented in Section 4 and its convergence analysis is given in Section 5.

The advantage of our new approach over the algorithms in [CF04, KMSS12] is twofold. First, from the fact that the TAFEM aims in an equal distribution of the error, we expect an improved performance. Second, we use an L^2-strategy for the consistency error, which requires only L^2-regularity of f in time in stead of the H^1-regularity needed for the L^∞-strategy in [CF04, KMSS12]. This makes the proposed method suitable for problems, where the existing approaches may even fail completely. We conclude the paper in Section 6 by comments on the implementation in DUNE [BBD+16] and some numerical experiments. The experiments confirm the expectations and show a more than competitive performance of our algorithm TAFEM.

2. The Continuous and Discrete Problems

In this section, we state the weak formulation of the continuous problem together with the assumptions on data. Then the discretisation by adaptive finite elements in space combined with the dG(s) scheme in time is introduced.

2.1. The Weak Formulation.

For $d \in \mathbb{N}$, let $\Omega \subset \mathbb{R}^d$ be a bounded, polyhedral domain that is meshed by some conforming simplicial mesh $\mathcal{G}_{\text{init}}$. We denote by $H^1(\Omega)$ the Sobolev space of square integrable functions $L^2(\Omega)$ whose first derivatives are in $L^2(\Omega)$ and we let $\mathbb{V} := H^1_0(\Omega)$ be the space of functions in $H^1(\Omega)$ with vanishing trace on $\partial\Omega$. For any measurable set ω and $k \in \mathbb{N}$, we denote by $\|\cdot\|_\omega$ the $L^2(\omega;\mathbb{R}^k)$ norm, whence $\|v\|^2_{H^1(\Omega)} = \|v\|^2_\Omega + \|\nabla v\|^2_\Omega$.

We suppose that the data of (1.1) has the following properties: $\mathbf{A} : \Omega \to \mathbb{R}^{d\times d}$ is piecewise Lipschitz over $\mathcal{G}_{\text{init}}$ and is symmetric positive definite with eigenvalues $0 < a_* \leqslant a^* < \infty$, i. e.,

$$a_*|\boldsymbol{\xi}|^2 \leqslant \mathbf{A}(x)\boldsymbol{\xi}\cdot\boldsymbol{\xi} \leqslant a^*|\boldsymbol{\xi}|^2, \qquad \text{for all } \boldsymbol{\xi}\in\mathbb{R}^d,\ x\in\Omega, \tag{2.1}$$

$c \in L^\infty(\Omega)$ is non-negative, i. e., $c \geqslant 0$ in Ω, $f \in L^2((0,T);L^2(\Omega)) = L^2(\Omega\times(0,T))$, and $u_0 \in L^2(\Omega)$.

We next turn to the weak formulation of (1.1); compare with [Eva10, Chap. 7]. We let $\mathcal{B} : \mathbb{V}\times\mathbb{V}\to\mathbb{R}$ be the symmetric bilinear form associated to the weak form of elliptic operator $\mathcal{L}$, i. e.,

$$\mathcal{B}[w,\,v] := \int_\Omega \mathbf{A}\nabla v\cdot\nabla w + c\,vw\,dV \qquad \text{for all } v,\,w\in\mathbb{V}.$$

Recalling the Poincaré-Friedrichs inequality $\|v\|_\Omega \leqslant C(d,\Omega)\|\nabla v\|_\Omega$ for all $v\in\mathbb{V}$ [GT01, p. 158] we deduce from (2.1) that $\mathcal{B}$ is a scalar product on $\mathbb{V}$ with induced norm

$$|\!|\!|v|\!|\!|_\Omega^2 := \mathcal{B}[v,\,v] = \int_\Omega \mathbf{A}\nabla v\cdot\nabla v + cv^2\,dV \qquad \text{for all } v\in H^1_0(\Omega).$$

This *energy norm* is equivalent to the H^1-norm $\|\cdot\|_{H^1(\Omega)}$ and we shall use the energy norm in the subsequent analysis. We denote the restriction of the energy norm to some subset $\omega\subset\Omega$ by $|\!|\!|\cdot|\!|\!|_\omega$ and let $\mathbb{V}^* := H^{-1}(\Omega)$ be the dual space of $H^1_0(\Omega)$ equipped with the operator norm $|\!|\!|g|\!|\!|_* := \sup_{v\in\mathbb{V}} \frac{\langle g,\,v\rangle}{|\!|\!|v|\!|\!|_\Omega}$.

The weak solution space

$$\mathbb{W}(0,T) := \left\{u\in L^2(0,T;\mathbb{V}) \mid \partial_t u\in L^2(0,T;\mathbb{V}^*)\right\}.$$

is a Banach space endowed with the norm

$$\|v\|^2_{\mathbb{W}(0,T)} = \int_0^T |\!|\!|\partial_t v|\!|\!|_*^2 + |\!|\!|v|\!|\!|_\Omega^2\,\mathrm{d}t + \|v(T)\|_\Omega^2, \qquad v\in\mathbb{W}(0,T).$$

Moreover, it is continuously embedded into $C^0([0,T];L^2(\Omega))$; see e.g. [Eva10, Chap. 5].

After these preparations, we are in the position to state the weak formulation of (1.1): A function $u\in\mathbb{W}(0,T)$ is a weak solution to (1.1) if it satisfies

$$\langle\partial_t u(t),\,v\rangle + \mathcal{B}[u(t),\,v] = \langle f(t),\,v\rangle_\Omega \quad \text{for all } v\in\mathbb{V},\ \text{a.e. } t\in(0,T), \tag{2.2a}$$

$$u(0) = u_0. \tag{2.2b}$$

Hereafter, $\langle\cdot,\cdot\rangle_\Omega$ denotes the $L^2(\Omega)$ scalar product. Since the operator $\mathcal{L}$ is elliptic, problem (2.2) admits for any $f\in L^2(0,T;L^2(\Omega))$ and $u_0\in L^2(\Omega)$ a unique weak solution; compare e.g. with [Eva10, Chap. 7].

2.2. **The Discrete Problem.** For the discretization of (2.2) we use adaptive finite elements in space and a dG(s) scheme with adaptive time-step-size controle.

Adaptive Grids and Time Steps. For the adaptive space discretization we restrict ourselves to simplicial grids and local refinement by bisection; compare with [Bän91, Kos94, Mau95, Tra97] as well as [NSV09, SS05] and the references therein. To be more precise, refinement is based on the initial conforming triangulation $\mathcal{G}_{\text{init}}$ of Ω and a procedure `REFINE` with the following properties. Given a conforming triangulation $\mathcal{G}$ and a subset $\mathcal{M}\subset\mathcal{G}$ of *marked elements*. Then

$$\texttt{REFINE}(\mathcal{G},\mathcal{M})$$

outputs a conforming refinement $\mathcal{G}_+$ of $\mathcal{G}$ such that all elements in $\mathcal{M}$ are bisected at least once. In general, additional elements are refined in order to ensure conformity. The input $\mathcal{G}$ can either be $\mathcal{G}_{\text{init}}$ or the output of a previous application of `REFINE`. The class of all conforming triangulations that can be produced from $\mathcal{G}_{\text{init}}$ by finite many applications of `REFINE`, we denote by $\mathbb{G}$. For $\mathcal{G}\in\mathbb{G}$ we call $\mathcal{G}_+\in\mathbb{G}$ a

refinement of $\mathcal{G}$ if $\mathcal{G}_+$ is produced from $\mathcal{G}$ by a finite number of applications of `REFINE` and we denote this by $\mathcal{G} \leqslant \mathcal{G}_+$ or $\mathcal{G}_+ \geqslant \mathcal{G}$. Conversely, we call any $\mathcal{G}_- \in \mathbb{G}$ with $\mathcal{G}_- \leqslant \mathcal{G}$ a *coarsening* of $\mathcal{G}$.

Throughout the discussion we only deal with conforming grids, this means, whenever we refer to some triangulations $\mathcal{G}$, $\mathcal{G}_+$, and $\mathcal{G}_-$ we tacitly assume $\mathcal{G}, \mathcal{G}_+, \mathcal{G}_- \in \mathbb{G}$. One key property of the refinement by bisection is uniform shape regularity for any $\mathcal{G} \in \mathbb{G}$. This means that all constants depending on the shape regularity are uniformly bounded depending on $\mathcal{G}_{\text{init}}$.

For the discretization in time we let $0 = t_0 < t_1 < \cdots < t_N = T$ be a partition of $(0,T)$ into half open subintervals $I_n = (t_{n-1}, t_n]$ with corresponding local time-step sizes $\tau_n := |I_n| = t_n - t_{n-1}$, $n = 1, \dots, N$.

Space-Time Discretization. For the spatial discretization we use Lagrange finite elements. This is, for any $\mathcal{G} \in \mathbb{G}$ the finite element space $\mathbb{V}(\mathcal{G})$ consists of all continuous, piecewise polynomials of fixed degree $\ell \geqslant 1$ over $\mathcal{G}$ that vanish on $\partial\Omega$. This gives a conforming discretization of $\mathbb{V}$, i. e., $\mathbb{V}(\mathcal{G}) \subset \mathbb{V}$. Moreover, Lagrange finite elements give nested spaces, i. e., $\mathbb{V}(\mathcal{G}) \subset \mathbb{V}(\mathcal{G}_+)$ whenever $\mathcal{G} \leqslant \mathcal{G}_+$.

We denote by $\mathcal{G}_0$ the triangulation at $t_0 = 0$ and for $n \geqslant 1$, we denote by $\mathcal{G}_n$ the grid in I_n and let $\mathbb{V}_n = \mathbb{V}(\mathcal{G}_n)$, $n = 0, \dots, N$, be the corresponding finite element spaces. For $\mathcal{G} \in \mathbb{G}$ we denote by $\Pi_{\mathcal{G}} \colon L^2(\Omega) \to \mathbb{V}(\mathcal{G})$ the L^2 projection onto $\mathbb{V}(\mathcal{G})$ and set $\Pi_n := \Pi_{\mathcal{G}_n}$.

On each time interval, the discrete approximation is polynomial in time over the corresponding spatial finite element space. Let $s \in \mathbb{N}_0$, for any real vector space $\mathbb{U}$ and interval $I \subset \mathbb{R}$, we denote by

$$\mathbb{P}_s\big(I, \mathbb{U}\big) := \Big\{ t \mapsto \sum_{i=0}^{s} t^i V_i : V_i \in \mathbb{U} \Big\}$$

the space of all polynomials with degree less or equal s over $\mathbb{U}$. We write $\mathbb{P}_s(\mathbb{U}) := \mathbb{P}_s(\mathbb{R}, \mathbb{U})$ and $\mathbb{P}_s := \mathbb{P}_s(\mathbb{R})$.

Furthermore, for an interval $I \subset (0,T)$ we let

$$f_I \in \mathbb{P}_s(I, L^2(\Omega))$$

be the best-approximation of $f_{|I}$ in $L^2(I, L^2(\Omega))$. In particular we use $f_n := f_{I_n}$ as a time-discretization of f on I_n. For $s = 0$, $f_I = \fint_I f \,\mathrm{d}t$ is the mean value of f on I.

In the following, we introduce the so called discontinuous Galerkin time-stepping scheme dG(s) of degree s, where dG(0) is the well know implicit Euler scheme. To this end, we denote for $n \geqslant 1$ the actual grid on I_n by $\mathcal{G}_n$ and let $\mathbb{V}_n = \mathbb{V}(\mathcal{G}_n)$ be the corresponding finite element space. We start with a suitable initial refinement $\mathcal{G}_0$ of $\mathcal{G}_{\text{init}}$ and an approximation $U_0 = \Pi_0 u_0 = \Pi_{\mathcal{G}_0} u_0 \in \mathbb{V}_0$ of the initial value u_0. Note that in principle, any suitable interpolation operator can be used instead of Π_0. We then inductively compute for $n > 0$ a solution $U_{|I_n} \in \mathbb{P}_s(\mathbb{V}_n)$ to the problem

$$\int_{I_n} \big\langle \partial_t U_{|I_n}, V \big\rangle_\Omega + \mathcal{B}[U_{|I_n}, V] \,\mathrm{d}t + \big\langle [\![U]\!]_{n-1}, V(t_{n-1}) \big\rangle_\Omega = \int_{I_n} \langle f_n, V \rangle_\Omega \,\mathrm{d}t \quad (2.3)$$

for all $V \in \mathbb{P}_s(\mathbb{V}_n)$. Thereby $f_n := f_{I_n}$ and $[\![U]\!]_{n-1}$ denotes the jump

$$[\![U]\!]_{n-1} := U_{n-1}^+ - U_{n-1}^-,$$

of U across t_{n-1}, where we used $U_{n-1}^+ := \lim_{t \downarrow t_{n-1}} U_{|I_n}(t)$, $U_n^- := U_{|I_n}(t_n)$, $n = 1, \dots, N$, and $U_0^- := U_0$. Note that with this definition we have $U_{n-1}^- = U(t_{n-1})$. The solution U is uniquely defined [Tho06] and we will see below that (2.3) is equivalent to an $s+1$ dimensional second order elliptic system. Note that U is allowed to be discontinuous across the nodal points $t_0, \dots, t_N$ and hence in general $U \notin \mathbb{W}(0,T)$.

In order to construct from U a conforming function, we recall that the dG(s) schemes are closely related to Runge Kutta RadauIIA collocation methods; see e.g. [AMN09]. The corresponding RadauIIA quadrature formula with abscissae $c_1, \dots, c_{s+1}$ and weights $b_1, \dots, b_{s+1}$ is exact of degree $2s$. In fact, we have

$$\sum_{j=1}^{s+1} b_j P(c_j) = \int_0^1 P(t)\,\mathrm{d}t \qquad \text{for all } P \in \mathbb{P}_{2s}. \tag{2.4}$$

We define $\mathcal{U} \in \mathbb{W}(0,T)$, $\mathcal{U}_{|I_n} \in \mathbb{P}_{s+1}(\mathbb{V})$ as the piecewise interpolation of U at the local RadauIIA points $t_n^j := t_{n-1} + c_j\tau_n$, i. e.,

$$\mathcal{U}(t_n^j) = U_{|I_n}(t_n^j) \in \mathbb{V}_n, \qquad j = 1, \dots, s+1. \tag{2.5a}$$

The continuous embedding of $\mathbb{W}(0,T)$ in $C^0([0,T]; L^2(\Omega))$ additionally enforces

$$\mathcal{U}(t_{n-1}) = U_{n-1}^- \in \mathbb{V}_{n-1}. \tag{2.5b}$$

Hence $\mathcal{U}$ is uniquely defined by

$$\mathcal{U}_{|I_n} := \sum_{j=0}^{s+1} L_j\big(\tfrac{t-t_{n-1}}{\tau_n}\big)\, U(t_n^j); \tag{2.6}$$

with the Lagrange polynomials

$$L_j(t) := \prod_{\substack{i=0 \\ i\neq j}}^{s+1} \frac{t-c_j}{c_i-c_j} \in \mathbb{P}_{s+1}, \qquad j = 0, \dots, s+1 \tag{2.7}$$

and $c_0 := 0$. Using integration by parts with respect to time, (2.4), and (2.5), we observe that (2.3) is equivalent to

$$\int_{I_n} \langle \partial_t \mathcal{U}, V\rangle_\Omega + \mathcal{B}[U, V]\,\mathrm{d}t = \int_{I_n} \langle f_n, V\rangle_\Omega \,\mathrm{d}t \tag{2.8}$$

for all $n = 1, \dots, n$ and $V \in \mathbb{P}_s(\mathbb{V}_n)$.

We emphasize that $\mathcal{U}(t)$ is a finite element function, since for $t \in I_n$, we have $\mathcal{U}(t) \in \mathbb{V}(\mathcal{G}_{n-1} \oplus \mathcal{G}_n) \subset \mathbb{V}$, where $\mathcal{G}_{n-1} \oplus \mathcal{G}_n$ is the smallest common refinement of $\mathcal{G}_{n-1}$ and $\mathcal{G}_n$, which we call *overlay*. Continuity of $\mathcal{U}$ in time, in combination with $\mathcal{U}(t) \in \mathbb{V}$ for all $t \in I$ then implies $\mathcal{U} \in \mathbb{W}(0,T)$.

Remark 1. *For $s = 0$ we see from* (2.3) *that in each time-step $n \in \mathbb{N}$, we need to solve for partial differential operators of the form $-\Delta + \mu$ with $\mu = \frac{1}{\tau_n}$ in order to compute U_n. Unfortunately, for $s > 0$, though still coercive,* (2.3) *becomes a $s+1$ dimensional coupled non-symmetric system. Recently, in* [Sme15] *a PCG method for a symmetrisation of* (2.3) *is proposed, which is fully robust with respect to the discretisation parameters s and τ, provided a solver for the operator $-\Delta + \mu$, $\mu \geqslant 0$ is available.*

3. A Posteriori Error Estimation

One basic ingredient of adaptive methods are a posteriori error indicators building up a reliable upper bound for the error in terms of the discrete solution and given data. The dG(0) method corresponds to the implicit Euler scheme and residual based estimators for the heat equation can be found in [Ver03]. In this section we generalize this result and prove reliable and efficient residual based estimators for dG(s) schemes (2.3), with arbitrary $s \in \mathbb{N}_0$.

Some arguments in this section are straight forward generalizations of those in [Ver03] and we only sketch their proofs, others are based on new ideas and therefore we shall prove them in detail.

3.1. **Equivalence of Error and Residual.** In order to prove residual based error estimators, one first has to relate the error to the residual. To this end we note that (2.2) can be taken as an operator equation in $L^2(0,T;\mathbb{V}^*) \times L^2(\Omega)$. Its residual $\mathrm{Res}(\mathcal{U})$ in $\mathcal{U} \in \mathbb{W}(0,T)$ is given by

$$\begin{aligned} \langle \mathrm{Res}(\mathcal{U}),\, v\rangle &= \langle \partial_t(u-\mathcal{U}),\, v\rangle + \mathcal{B}[u-\mathcal{U},\, v] \\ &= \langle f - \partial_t \mathcal{U},\, v\rangle_\Omega - \mathcal{B}[\mathcal{U},\, v] \qquad \text{for all } v \in \mathbb{V}. \end{aligned} \tag{3.1}$$

From [TV16], we have the following identity between the residual and the error.

Proposition 2 (Abstract Error Bound)**.** *Let $u \in \mathbb{W}(0,T)$ be the solution of* (2.2) *and let $\mathcal{U} \in \mathbb{W}(0,T)$ be the approximation defined in* (2.5) *for time instances $t_0 = 0, \dots, t_N = T$ and time-step sizes $\tau_n := t_n - t_{n-1}$, $n = 1, \dots, N$. Then it holds for $0 \leqslant k \leqslant N$, that*

$$\|u-\mathcal{U}\|^2_{\mathbb{W}(0,T)} = \|u_0 - U_0\|^2_\Omega + \|\,\mathrm{Res}(\mathcal{U})\|^2_{L^2(0,T;\mathbb{V}*)} \tag{3.2a}$$

and

$$\|\,\mathrm{Res}(\mathcal{U})\|^2_{L^2(I_n,\mathbb{V}*)} \leqslant 2\big\{\|\partial_t(u-\mathcal{U})\|^2_{L^2(I_n;\mathbb{V}*)} + \|u-\mathcal{U}\|^2_{L^2(I_n;\mathbb{V})}\big\}. \tag{3.2b}$$

The rest of this section concentrates on proving computable upper and lower bounds for the error. We note that the initial error $\|u_0 - U_0\|_\Omega$ in (3.2) is already a posteriori computable, whence it remains to estimate the dual norm of the residual. However, there is another issue of separating the influence of the temporal and the spatial discretization to the error. In particular, defining the temporal residual $\mathrm{Res}_\tau(\mathcal{U}) \in L^2(0,T;\mathbb{V}^*)$ as

$$\langle \mathrm{Res}_\tau(\mathcal{U}),\, v\rangle := \mathcal{B}[U-\mathcal{U},\, v] \tag{3.3}$$

and the spatial residual $\mathrm{Res}_h(\mathcal{U}) \in L^2(0,T;\mathbb{V}^*)$ as

$$\langle \mathrm{Res}_h(\mathcal{U}),\, v\rangle := \langle f_n - \partial_t \mathcal{U},\, v\rangle - \mathcal{B}[U,\, v] \qquad \text{on} \quad I_n, \tag{3.4}$$

we obtain

$$\mathrm{Res}(\mathcal{U}) = \mathrm{Res}_\tau(\mathcal{U}) + \mathrm{Res}_h(\mathcal{U}) + f - f_n \qquad \text{on} \quad I_n. \tag{3.5}$$

In what follows we use this decomposition to prove separated time and space error indicators, which build up a reliable and efficient bound for the error.

3.2. **Temporal Residual.** Recalling the definition of the Lagrange polynomials (2.7), we have the local unique representation

$$U_{|I_n}(t) = U^+_{n-1} L_0(\tfrac{t-t_{n-1}}{\tau_n}) + \sum_{j=1}^{s+1} U(t_n^j)\, L_j(\tfrac{t-t_{n-1}}{\tau_n}) \in \mathbb{P}_s(\mathbb{V}_n)$$

for all $t \in I_n$. Hence, by (2.6) we get

$$\mathcal{U}(t) - U(t) = (U^-_{n-1} - U^+_{n-1})\, L_0(\tfrac{t-t_{n-1}}{\tau_n})$$

and thanks to (2.5) and (2.4), we obtain

$$\begin{aligned} \int_{I_n} \|\,\mathrm{Res}_\tau(\mathcal{U})\|^2_{\mathbb{V}*}\,\mathrm{d}t &= \int_{I_n} |\!|\!| U-\mathcal{U} |\!|\!|^2_\Omega \,\mathrm{d}t = |\!|\!| U^-_{n-1} - U^+_{n-1} |\!|\!|^2_\Omega \int_{I_n} |L_0(\tfrac{t-t_{n-1}}{\tau_n})|^2\,\mathrm{d}t \\ &= \tau_n\, C_\tau\, |\!|\!| U^-_{n-1} - U^+_{n-1} |\!|\!|^2_\Omega, \end{aligned} \tag{3.6}$$

where $C_\tau = C_\tau(s) := \int_0^1 |L_0(t)|^2\,\mathrm{d}t$.

Remark 3. *Observing that the RadauIIA abscissae are the roots of the polynomial* $\lambda_s(2t-1) - \lambda_{s+1}(2t-1)$ *and* $\lambda_s(-1) = (-1)^s$*, with the Legendre polynomials* λ_n*,* $n \in \mathbb{N}_0$*, it follows that we have the representation*

$$L_0(t) = \frac{(-1)^s}{2}(\lambda_s(2t-1) - \lambda_{s+1}(2t-1))$$

and it can be easily shown that $C_\tau = \frac{1}{4}(\frac{1}{2s+3} + \frac{1}{2s+1})$*.*

3.3. **The Spatial Residual.** In this section we estimate the spatial residual.

Lemma 4. *Let* U *be the approximation of* (2.3) *to the solution* u *of* (2.2) *and let* $\mathcal{U}$ *be its interpolation defined by* (2.5)*. Then there exists a constant* $C_{\mathbb{G}} > 0$*, such that*

$$\int_{I_n} \|\operatorname{Res}_h(\mathcal{U})\|_{\mathbb{V}*}^2 \,\mathrm{d}t \leqslant C_{\mathbb{G}} \sum_{E\in\mathcal{G}_n} \int_{I_n} h_E^2 \|\partial_t \mathcal{U} + \mathcal{L}U - f_n\|_E^2 + h_E \|J(U)\|_{\partial E}^2 \,\mathrm{d}t$$

for all $1 \leqslant n \leqslant N$*. Thereby, for* $V \in \mathbb{V}_n$ *we denote by* $J(V)|_S$ *for an interior side* S *the jump of the normal flux* $\mathbf{A}\nabla V \cdot \boldsymbol{n}$ *across* S *and for boundary sides* S *we set* $J(V)|_S \equiv 0$*. The mesh-size of an element* $E \in \mathcal{G}$ *is given by* $h_E := |E|^{1/d}$*.*

Proof. Recalling (3.4), we first observe that $\|\operatorname{Res}_h(\mathcal{U})\|_{\mathbb{V}*}^2 \in \mathbb{P}_{2s}$, whence by (2.4) we have

$$\int_{I_n} \|\operatorname{Res}_h(\mathcal{U})\|_{\mathbb{V}*}^2 \,\mathrm{d}t = \tau_n \sum_{j=1} b_j \|\operatorname{Res}_h(\mathcal{U})(t_n^j)\|_{\mathbb{V}*}^2.$$

Therefore, it suffices to estimate $\|\operatorname{Res}_h(\mathcal{U})\|_{\mathbb{V}*}^2$ at the abscissae of the RadauIIA quadrature formula. For arbitrary $V_j \in \mathbb{V}_n$, $j = 1, \ldots, s+1$ choose $V \in \mathbb{P}_s(\mathbb{V}_n)$ in (2.8) such that $V(t + c_i\tau_n) = V_j\delta_{ij}$, $1 \leqslant i \leqslant s+1$. Then exploiting again (2.4) yields the Galerkin orthogonality

$$\big\langle \operatorname{Res}_h(\mathcal{U})(t_n^j),\, V_j \big\rangle = 0 \qquad j = 1, \ldots, s+1.$$

Since $V_j \in \mathbb{V}_n$ was arbitrary, we have for any $v \in \mathbb{V}$, that

$$\big\langle \operatorname{Res}_h(\mathcal{U})(t_n^j),\, v \big\rangle = \big\langle \operatorname{Res}_h(\mathcal{U})(t_n^j),\, v - V \big\rangle \qquad \text{for all } V \in \mathbb{V}_n.$$

Using integration by parts with respect to the space variable, the Cauchy-Schwarz inequality, the scaled trace inequality, and choosing V as a suitable interpolation of v, we arrive at

$$\|\operatorname{Res}_h(\mathcal{U})(t_n^j)\|_{\mathbb{V}*}^2 \leqslant C_{\mathbb{G}} \sum_{E\in\mathcal{G}_n} \Big\{ h_E^2 \|(\partial_t \mathcal{U} + \mathcal{L}U - f_n)(t_n^j)\|_E^2 + h_E \|J(U)(t_n^j)\|_{\partial E}^2 \Big\}.$$

The right hand side is a pointwise evaluation of a polynomial of degree $2s$ and thus the claimed upper bound follows from (2.4). □

The following result shows that the spatial indicators are locally efficient as well.

Lemma 5. *Under the conditions of Lemma 4, we have*

$$\sum_{E\in\mathcal{G}_n} \int_{I_n} h_E^2 \|\partial_t \mathcal{U} + \mathcal{L}U - f_n\|_E^2 + h_E \|J(U)\|_{\partial E}^2 \,\mathrm{d}t \\ \leqslant C\Big\{ \int_{I_n} \|\operatorname{Res}_h(\mathcal{U})\|_{\mathbb{V}*}^2 + \operatorname{osc}_{\mathcal{G}_n}^2(f_n, \mathcal{U}) \,\mathrm{d}t \Big\},$$

where

$$\operatorname{osc}_{\mathcal{G}_n}^2(f_n, \mathcal{U}) := \sum_{E\in\mathcal{G}_n} h_E^2 \|\partial_t \mathcal{U} + \mathcal{L}U - f_n - R_E\|_E^2 + h_E \|J(U) - J_E\|_{\partial E}^2$$

with at time $t \in I_n$ *pointwise* $L^2(\Omega)$*-best approximations* $R_E(t) \in \mathbb{P}_{2\ell-2}(E)$ *respectively* $J_E(t)_{|S} \in \mathbb{P}_{2\ell-1}(S)$ *for each side* $S \subset \partial E$*. The constant* $C > 0$ *depends solely on the shape regularity of* $\mathbb{G}$*.*

Proof. With the same arguments as in the proof of Lemma 4, for each $1 \leqslant j \leqslant s+1$ it suffices to prove that

$$C_{\mathbb{G}} \sum_{E\in\mathcal{G}_n} h_E^2 \|(\partial_t \mathcal{U} + \mathcal{L}U - f_n)(t_n^j)\|_E^2 + h_E \|J(U)(t_n^j)\|_{\partial E}^2 \\ \leqslant C\big\{\|\operatorname{Res}_h(\mathcal{U})(t_n^j)\|_{\mathbb{V}*}^2 + \operatorname{osc}_{\mathcal{G}_n}^2(f_n, U)(t_n^j)\big\}$$

This however, follows with standard techniques used in a posteriori estimation of elliptic second order problems; see e.g. [Ver13, MN05] and compare with the case of the implicit Euler scheme $s = 0$ in [Ver03]. □

3.4. **Estimation of the Error.** By means of the decomposition of the residual (3.5), we can combine the above results to obtain a reliable and efficient error estimator for (1.1). To this end, we introduce the following error indicators for the sake of brevity of presentation: For $\mathcal{G} \in \mathbb{G}$ and $v \in \mathbb{V}$, the estimator for the initial value is given by

$$\mathcal{E}_0^2(v, \mathcal{G}) := \|v - \mathcal{I}_{\mathcal{G}} v\|_\Omega^2 \tag{3.7a}$$

For $f \in L^2(0,T;L^2(\Omega))$, $t_\star \in (0,T)$ and $I = (t_\star, t_\star + \tau] \subset (t_\star, T]$, the so called consistency error, which is inherited by the decomposition of the residual (3.5) is defined by

$$\mathcal{E}_f^2(f, t_\star, \tau) := 3 \inf_{\bar f \in \mathbb{P}_s(L^2(\Omega))} \int_I \|f - \bar f\|_\Omega^2 \,\mathrm{d}t. \tag{3.7b}$$

For $v^-, v^+ \in \mathbb{V}$, $\mathcal{G} \in \mathbb{G}$, $V \in \mathbb{P}_s(\mathbb{V}(\mathcal{G}))$, $E \in \mathcal{G}$, and $g \in \mathbb{P}_s(L^2(\Omega))$ the indicator

$$\mathcal{E}_{c\tau}^2(v^+, v^-, \tau) := \tau\, 3\, C_\tau \,|\!|\!| v^- - v^+ |\!|\!|_\Omega^2 \tag{3.7c}$$

is motivated by (3.6) and Lemma 4 suggests to define the spatial indicators by

$$\begin{aligned}\mathcal{E}_{\mathcal{G}}^2(V, v^-, t_\star, \tau, g, \mathcal{G}, E) &:= 3\, C_{\mathbb{G}} \int_I h_E^2 \|\partial_t \mathcal{V} + \mathcal{L}V - g\|_E^2 + h_E \|J(V)\|_{\partial E}^2 \,\mathrm{d}t \\ &= 3\, C_{\mathbb{G}}\, \tau \sum_{j=1}^{s+1} b_j \Big\{ h_E^2 \|(\partial_t \mathcal{V} + \mathcal{L}V - g)(t_\star + c_j\tau)\|_E^2 \\ &\qquad + h_E \|J(V)(t_\star + c_j\tau)\|_{\partial E}^2 \Big\}.\end{aligned} \tag{3.7d}$$

Here we have used, analogously to (2.6), that

$$\mathcal{V}(t) := \sum_j^{s+1} L_j\big(\tfrac{t-t_\star}{\tau}\big)\, V(t_\star + c_j\tau) + L_0\big(\tfrac{t-t_\star}{\tau}\big) v^- \in \mathbb{P}_{s+1}(\mathbb{V}). \tag{3.8}$$

Proposition 6 (Upper Bound)**.** *Let $u \in \mathbb{W}(0,T)$ be the solution of (2.2) and let $\mathcal{U} \in \mathbb{W}(0,T)$ be the approximation defined in (2.5) for time instances $t_0 = 0, \dots, t_N = T$ and time-step sizes $\tau_n := t_n - t_{n-1}$, $n = 1, \dots, N$. Then we have the estimate*

$$\|u - \mathcal{U}\|_{\mathbb{W}(0,T)}^2 \leqslant \mathcal{E}_0^2(u_0, \mathcal{G}_0) + \sum_{n=1}^N \Big\{ \mathcal{E}_{c\tau}^2(U_{n-1}^+, U_{n-1}^-, \tau_n) \\ + \mathcal{E}_{\mathcal{G}}^2(U, U_{n-1}^-, t_n, \tau_n, f_n, \mathcal{G}_n) + \mathcal{E}_f^2(f, t_{n-1}, \tau_n) \Big\}.$$

Proof. By the decomposition of the residual (3.5) and the triangle inequality, we estimate on each interval I_n, $n = 1, \dots, N$

$$\|\operatorname{Res}(\mathcal{U})\|_{L^2(I_n;\mathbb{V}*)}^2 \leqslant 3\|\operatorname{Res}_\tau(\mathcal{U})\|_{L^2(I_n;\mathbb{V}*)}^2 + 3\|\operatorname{Res}_h(\mathcal{U})\|_{L^2(I_n;\mathbb{V}*)}^2 \\ + 3\|f - f_n\|_{L^2(I_n;\mathbb{V}*)}^2.$$

Now the assertion follows by Proposition 2, (3.6), and Lemma 4. □

Proposition 7 (Lower Bound)**.** *Supposing the conditions of Proposition 6, we have*

$$\begin{aligned}\mathcal{E}^2_{c\tau}(U^+_{n-1},U^-_{n-1},\tau_n)+\mathcal{E}^2_{\mathcal{G}}(U,U^-_{n-1},t_n,\tau_n,f_n,\mathcal{G}_n)\\ \leqslant C\Big\{\|\partial_t(u-\mathcal{U})\|^2_{L^2(I_n;\mathbb{V}*)}+\|u-\mathcal{U}\|^2_{L^2(I_n;\mathbb{V})}\\ +\int_{I_n}\operatorname{osc}^2_{\mathcal{G}_n}(f_n,\mathcal{U})\,\mathrm{d}t+\mathcal{E}^2_f(f,t_{n-1},\tau_n)\Big\},\end{aligned}$$

where the constant C depends solely on the shape regularity of $\mathbb{G}$ and on s.

Proof. We first consider the spatial indicators. By Lemma 5 there exists $C>0$, such that

$$\mathcal{E}^2_{\mathcal{G}}(U,U^-_{n-1},t_n,\tau_n,f_n,\mathcal{G}_n)\leqslant C\|\operatorname{Res}_h(\mathcal{U})\|^2_{L^2(I_n;\mathbb{V}*)}+C\int_{I_n}\operatorname{osc}^2_{\mathcal{G}_n}(f_n,\mathcal{U})\,\mathrm{d}t.$$

The first term on the right hand side can be further estimated using the decomposition of the residual, the triangle inequality, and (3.6) to obtain

$$\begin{aligned}\|\operatorname{Res}_h(\mathcal{U})\|_{L^2(I_n;\mathbb{V}*)}\leqslant\|\operatorname{Res}(\mathcal{U})\|_{L^2(I_n;\mathbb{V}*)}+\|f-f_n\|_{L^2(I_n;\mathbb{V}*)}\\ +\mathcal{E}_{c\tau}(U^-_{n-1},U^+_{n-1},\tau_n).\end{aligned}\tag{3.9}$$

It remains to bound the temporal estimator. To this end, we introduce a non-trivial auxiliary function $\alpha\in\mathbb{P}_{2s+2}$ such that $\alpha\perp\mathbb{P}_{2s+1}$ and

$$\int_0^1 L_0^2(t)\,\alpha(t)\,\mathrm{d}t=1,$$

which is possible since $L_0^2\in\mathbb{P}_{2s+2}\backslash\mathbb{P}_{2s+1}$. Recalling (3.6), (3.3), and (3.5), we have for $\alpha_n(t):=\alpha\big(\frac{t-t_{n-1}}{\tau_n}\big)$ that

$$\begin{aligned}\mathcal{E}^2_{c\tau}(U^+_{n-1},U^-_{n-1},\tau_n)&=C_\tau|\!|\!|U^+_{n-1}-U^-_{n-1}|\!|\!|^2_\Omega\int_{I_n}L_0^2\big(\tfrac{t-t_{n-1}}{\tau_n}\big)\,\alpha_n(t)\,\mathrm{d}t\\ &=C_\tau\int_{I_n}\alpha_n\,\langle\operatorname{Res}(\mathcal{U}),U-\mathcal{U}\rangle-\alpha_n\,\langle f-f_n,U-\mathcal{U}\rangle_\Omega\,\mathrm{d}t\\ &\quad-C_\tau\int_{I_n}\alpha_n\,\langle\operatorname{Res}_h(\mathcal{U}),U-\mathcal{U}\rangle\,\mathrm{d}t.\end{aligned}$$

The last term vanishes since $\langle\operatorname{Res}_h(\mathcal{U}),U-\mathcal{U}\rangle\in\mathbb{P}_{2s+1}$. Using the Cauchy Schwarz and Young inequalities, we can hence estimate

$$\mathcal{E}^2_{c\tau}(U^+_{n-1},U^-_{n-1},\tau_n)\leqslant 2C_\tau\|\alpha\|^2_{L^\infty(0,1)}\Big\{\|\operatorname{Res}(\mathcal{U})\|^2_{L^2(I_n;\mathbb{V}*)}+\|f-f_n\|^2_{L^2(I_n;\mathbb{V}*)}\Big\}.$$

Combining this with (3.9), we arrive at

$$\begin{aligned}\mathcal{E}^2_{c\tau}(U^+_{n-1},U^-_{n-1},\tau_n)+\mathcal{E}^2_{\mathcal{G}}(U,U^-_{n-1},t,\tau_n,f_n,\mathcal{G}_n)\\ \leqslant\Big(C\big(1+2\|\alpha\|^2_{L^\infty(0,1)}C_\tau\big)+2\|\alpha\|^2_{L^\infty(0,1)}C_\tau\Big)\\ \Big\{\|\operatorname{Res}(\mathcal{U})\|^2_{L^2(I_n;\mathbb{V}*)}+\|f-f_n\|^2_{L^2(I_n;\mathbb{V}*)}\Big\}.\end{aligned}\tag{3.10}$$

Together with Proposition 2 this is the desired estimate. □

Remark 8 (Implicit Euler)**.** *We emphasize that the proof of the lower bound Proposition 7 is slightly different from the one in* [Ver03] *and yields different constants also for the* dG(0) *scheme. To see this, we observe that the definition of α implies for $s=0$ that*

$$\alpha(t)=30(6t^2-6t+1),\qquad\textit{whence}\qquad\|\alpha\|_{L^\infty(0,1)}=30.$$

Therefore, we conclude for the constant in (3.10) *with* $C_\tau = \frac{1}{3}$ *from Remark 3, that*

$$C\big(1 + 2\|\alpha\|^2_{L^\infty(0,1)} C_\tau\big) + 2\|\alpha\|^2_{L^\infty(0,1)} C_\tau = 601\, C + 600,$$

where C *is the constant in the estimate of Lemma 5. In contrast to this, the techniques used in* [Ver03] *for the implicit Euler scheme yield the constant*

$$\big(1 + 7C_{\mathbb{G}}^{1/2}\big)^2\, C_{\mathbb{G}}^{1/2}\, C^{3/2}\, 12^2.$$

Remark 9 (Elliptic Problem)**.** *In case of the implicit Euler scheme* dG(0)*, it is well known, that in each time-step* $1 \leqslant n \leqslant N$, $U_{|I_n} \in \mathbb{P}_0(\mathbb{V}_n) = \mathbb{V}_n$ *is the Ritz approximation to a coercive elliptic problem. Moreover, the spatial estimators* (3.7d) *are the standard residual based estimators for this elliptic problem. This observation transfers to the* dG(s) *scheme for* $s \geqslant 1$*. To see this, we observe that (after transformation to the unit interval)* (2.3) *is a Galerkin approximation to the solution* $u_\tau \in \mathbb{P}_s(\mathbb{V})$ *of a problem of the kind*

$$\begin{aligned}\int_0^1 \frac{1}{\tau}\langle \partial_t u_\tau,\, v\rangle_\Omega + \mathcal{B}[u_\tau,\, v]\,\mathrm{d}t + \frac{1}{\tau}\langle u_\tau(0),\, v(0)\rangle_\Omega \\ = \int_0^1 \big\langle \bar f,\, v\big\rangle_\Omega\,\mathrm{d}t + \frac{1}{\tau}\big\langle v^-,\, v(0)\big\rangle_\Omega\end{aligned} \tag{3.11}$$

for all $v \in \mathbb{P}_s(\mathbb{V})$ *and some data* $\bar f \in \mathbb{P}_s(L^2(\Omega))$, $v^- \in L^2(\Omega)$, *and* $\tau > 0$*. The mappings* $v \mapsto v(0)$ *and* $v \mapsto \partial_t v$ *are linear and continuous on* $\mathbb{P}_s(\mathbb{V})$*, whence this equation can be taken as a vector valued linear variational problem of second order on* $\mathbb{V}^{s+1}$*. Testing with* $v = u_\tau$ *proves coercivity*

$$\begin{aligned}\int_0^1 \frac{1}{\tau}\langle \partial_t u_\tau,\, u_\tau\rangle_\Omega + \mathcal{B}[u_\tau,\, u_\tau]\,\mathrm{d}t + \frac{1}{\tau}\langle u_\tau(0),\, u_\tau(0)\rangle_\Omega \\ = \frac{1}{2\tau}\|u_\tau(0)\|^2_\Omega + \frac{1}{2\tau}\|u_\tau(1)\|^2_\Omega + \int_0^1 |\!|\!| u_\tau |\!|\!|^2_\Omega\,\mathrm{d}t.\end{aligned}$$

Obviously, its residual in $V \in \mathbb{P}_s(\mathbb{V})$ *is given by*

$$\langle \mathrm{Res}_h(\mathcal{V}),\, v\rangle = \big\langle \bar f - \partial_t \mathcal{V},\, v\big\rangle - \mathcal{B}[V,\, v], \quad v \in \mathbb{P}_s(\mathbb{V}),$$

where $\mathcal{V} \in \mathbb{P}_{s+1}(\mathbb{V})$ *is such that* $\mathcal{V}(c_j) = V(c_j)$, $j = 1, \dots, s$ *and* $\mathcal{V}(0) = v^-$*; compare with* (2.5)*. Thanks to Lemmas 4 and 5, for* $V \in \mathbb{P}_s(\mathbb{V}(\mathcal{G}))$, $\mathcal{G} \in \mathbb{G}$*, the standard residual based estimator for this problem is given by* $\mathcal{E}^2_{\mathcal{G}}(V, v^-, \tau, 0, \bar f, \mathcal{G})$*.*

Energy Estimation. We shall now generalise the energy estimate from [KMSS12] to higher order dG(s) schemes.

Proposition 10 (Uniform global energy estimate)**.** *Assume* $N \in \mathbb{N} \cup \{\infty\}$ *and arbitrary time instances* $0 = t_0 < \cdots < t_N \leqslant T$ *with time -step-sizes* $\tau_1, \dots, \tau_N > 0$*. Let* $U_0 = \Pi_0 u_0$ *and for* $1 \leqslant n \leqslant N$ *let* $U_{|I_n} \in \mathbb{P}_s(\mathbb{V}_n)$ *be the discrete solutions to* (2.3) *and let* $\mathcal{U} \in \mathbb{W}(0,T)$ *as defined in* (2.5)*. Then for any* $m = 1, \dots, N$ *we have*

$$\sum_{n=1}^m \|\partial_t \mathcal{U}\|^2_\Omega + |\!|\!| U^+_{n-1} - \Pi_n U^-_{n-1} |\!|\!|^2_\Omega + |\!|\!| U^-_n |\!|\!|^2_\Omega - |\!|\!| \Pi_n U^-_{n-1} |\!|\!|^2_\Omega \leqslant \sum_{n=1}^m \int_{I_n} \|f_n\|^2_\Omega\,\mathrm{d}t.$$

Proof. We choose $V := \Pi_n \partial_t \mathcal{U}_{|I_n} \in \mathbb{P}_s(\mathbb{V}_n)$ as a test function in (2.8) obtaining

$$\int_{I_n} \|\Pi_n \partial_t \mathcal{U}\|^2_\Omega + \mathcal{B}[U,\, \Pi_n \partial_t \mathcal{U}]\,\mathrm{d}t = \int_{I_n} \langle f_n,\, \Pi_n \partial_t \mathcal{U}\rangle_\Omega\,\mathrm{d}t. \tag{3.12}$$

In order to analyse the second term on the left hand side, we first observe that $\Pi_n \partial_t \mathcal{U}_{|I_n} = \partial_t \Pi_n \mathcal{U}_{|I_n} \in \mathbb{P}_s(\mathbb{V}_n)$. Recalling (2.5b) and that $\mathcal{B} : \mathbb{V} \times \mathbb{V} \to \mathbb{R}$ is constant in time, we obtain integrating by parts, that

$$\int_{I_n} \mathcal{B}[U,\, \Pi_n \partial_t \mathcal{U}]\,\mathrm{d}t = -\int_{I_n} \mathcal{B}[\partial_t U,\, \Pi_n \mathcal{U}]\,\mathrm{d}t + |\!|\!| U^-_n |\!|\!|^2_\Omega - \mathcal{B}[U^+_{n-1},\, \Pi_n U^-_{n-1}].$$

Since $\mathcal{B}[\partial_t U,\, \Pi_n \mathcal{U}]_{|I_n} \in \mathbb{P}_{2s}$, we can apply (2.4) and conclude with (2.5a) that

$$\begin{aligned}\int_{I_n} \mathcal{B}[U,\, \Pi_n \partial_t \mathcal{U}]\,\mathrm{d}t &= -\int_{I_n} \mathcal{B}[\partial_t U,\, U]\,\mathrm{d}t + \|U_n^-\|_\Omega^2 - \mathcal{B}[U_{n-1}^+,\, \Pi_n U_{n-1}^-] \\ &= \frac{1}{2}\|U_{n-1}^+ - \Pi_n U_{n-1}^-\|_\Omega^2 - \frac{1}{2}\|\Pi_n U_{n-1}^-\|_\Omega^2 + \frac{1}{2}\|U_n^-\|_\Omega^2,\end{aligned}$$

where we used that $\mathcal{B}[\partial_t U_{|I_n},\, U_{|I_n}] = \frac{1}{2}\partial_t \|U_{|I_n}\|_\Omega^2$. Inserting this in (3.12) yields

$$\begin{aligned}\int_{I_n} \|\Pi_n \partial_t \mathcal{U}\|_\Omega^2\,\mathrm{d}t + \frac{1}{2}\|U_{n-1}^+ - \Pi_n U_{n-1}^-\|_\Omega^2 - \frac{1}{2}\|\Pi_n U_{n-1}^-\|_\Omega^2 + \frac{1}{2}\|U_n^-\|_\Omega^2 \\ = \int_{I_n} \langle f_n,\, \Pi_n \partial_t \mathcal{U}\rangle_\Omega\,\mathrm{d}t.\end{aligned}$$

Estimating the right hand side with the help of the Cauchy-Schwarz and the Young inequality proves the assertion. □

Corollary 11. *Under the conditions of Proposition 10, assume that*

$$\|U_{n-1}^-\|_\Omega^2 - \|\Pi_n U_{n-1}^-\|_\Omega^2 + \frac{1}{2}\int_{I_n} \|\Pi_n \partial_t \mathcal{U}\|_\Omega^2\,\mathrm{d}t \geqslant 0 \quad \text{for} \quad n = 1, \dots, N. \tag{3.13}$$

Then we have the estimate

$$\sum_{n=1}^{m} \frac{1}{2}\int_{I_n} \|\Pi_n \partial_t \mathcal{U}\|_\Omega^2\,\mathrm{d}t + \|U_{n-1}^+ - \Pi_n U_{n-1}^-\|_\Omega^2 \leqslant \|f\|_{\Omega\times(0,t_m)}^2 + \|U_0\|_\Omega^2 - \|U_m^-\|_\Omega^2.$$

In particular, the series $\sum_{n=1}^{N} \|U_{n-1}^+ - \Pi_n U_{n-1}^-\|_\Omega^2$ *is uniformly bounded irrespective of the sequence of time-step-sizes used.*

Proof. Summing up the nonnegative terms in (3.13) yields

$$0 \leqslant \sum_{n=1}^{m} \|U_{n-1}^-\|_\Omega^2 - \|\Pi_n U_{n-1}^-\|_\Omega^2 + \frac{1}{2}\int_{I_n} \|\Pi_n \partial_t \mathcal{U}\|_\Omega^2\,\mathrm{d}t,$$

which is equivalent to

$$\|U_m^-\|_\Omega^2 - \|U_0\|_\Omega^2 \leqslant \sum_{n=1}^{m} \|U_{n-1}^+\|_\Omega^2 - \|\Pi_n U_{n-1}^-\|_\Omega^2 + \frac{1}{2}\int_{I_n} \|\Pi_n \partial_t \mathcal{U}\|_\Omega^2\,\mathrm{d}t.$$

Using this in the estimate of Proposition 10 yields the desired estimate. □

Having a closer look at the indicator $\mathcal{E}_{c\tau}$ we note that, since we allow for coarsening, it is not a pure temporal error indicator. Coarsening may cause the loss of information and to few information my lead to wrong decisions within the adaptive method. For this reason we use the triangle inequality to split

$$\mathcal{E}_{c\tau}^2(v^-, v^+, \tau, \mathcal{G}) \leqslant \mathcal{E}_c^2(v^-, \tau, \mathcal{G}) + \mathcal{E}_\tau^2(v^+, v^-, \tau, \mathcal{G}) \tag{3.14a}$$

into a measure

$$\mathcal{E}_c^2(v^-, \tau, \mathcal{G}) := \sum_{E\in\mathcal{G}} \mathcal{E}_c^2(v^-, \tau, \mathcal{G}, E) := 6\,C_\tau \sum_{E\in\mathcal{G}} \tau \|\Pi_{\mathcal{G}} v^- - v^-\|_E^2 \tag{3.14b}$$

for the coarsening error and

$$\mathcal{E}_\tau^2(v^+, v^-, \tau, \mathcal{G}) := 6\,C_\tau \tau \|v^+ - \Pi_{\mathcal{G}} v^-\|_\Omega^2, \tag{3.14c}$$

which serves as an indicator for the temporal error. This allows us to control the coarsening error separately.

Assuming that (3.13) holds, Corollary 11 provides control of the sum of the time error indicators $\mathcal{E}_\tau^2(U_{n-1}^+, U_{n-1}^-, \tau_n, \mathcal{G}_n) = 6C_{c\tau}\tau \|U_{n-1}^+ - \Pi_n U_{n-1}^-\|_\Omega^2$. Assumption (3.13) would trivially be satisfied for the Ritz-projection $R_n U_{n-1}^-$ of U_{n-1}^- into $\mathbb{V}_n$, since $\|R_n U_{n-1}^-\|_\Omega \leqslant \|U_{n-1}^-\|_\Omega$. The L^2-projection $\Pi_n U_{n-1}^-$, however, does not satisfy

this monotonicity property in general and therefore coarsening may lead to an increase of energy. The algorithm presented below ensures that (3.13) is fulfilled at the end of every time-step. To this end, using the notation (3.8), we define for $V \in \mathbb{P}_s(\mathbb{V}(\mathcal{G}))$, $v^- \in \mathbb{V}$, $t_\star \in (0,T)$, $I = (t_\star, t_\star + \tau] \subset (t_\star, T]$, $\mathcal{G} \in \mathbb{G}$, and $E \in \mathcal{G}$, the indicators

$$\mathcal{E}_*^2(V, v^-, t_\star, \tau, \mathcal{G}, E) := \left\|\Pi_{\mathcal{G}} v^-\right\|_E^2 - \left\|v^-\right\|_E^2 - \frac{1}{2}\int_I \|\Pi_{\mathcal{G}} \partial_t \mathcal{V}\|_E^2 \,\mathrm{d}t,$$

as well as the convenient notation $\mathcal{E}_*^2(V, v^-, t_\star, \tau, \mathcal{G}) := \sum_{E\in\mathcal{G}} \mathcal{E}_*^2(V, v^-, t_\star, \tau, \mathcal{G}, E)$. Condition (3.13) is then equivalent to $\mathcal{E}_*^2(U, U_{n-1}^-, t_{n-1}, \tau_n, \mathcal{G}_n) \leqslant 0$, $n = 1, \dots, N$. Note that the term $-\int_{I_n} \|\Pi_{\mathcal{G}} \partial_t \mathcal{V}\|_E^2$ may compensate for $\left\|\Pi_{\mathcal{G}} v^-\right\|_E^2 > \left\|v^-\right\|_E^2$.

4. The adaptive algorithm TAFEM

Based on the observations in the previous section and a new concept for marking we shall next describe the adaptive algorithm TAFEM in this section. In contrast to the algorithms presented in [KMSS12] and [CF04], the TAFEM is based on a different marking philosophy. In fact, they mark according to the same indicators, (3.7b)-(3.7d) and (3.14), but in contrast to [KMSS12, CF04], the TAFEM uses an L^2 instead of an L^∞ strategy. Philosophically, this aims at an L^2 rather than an L^∞ equal-distribution of the error in time; compare also with the introductory section 1.

We follow a bottom up approach, i.e., we first state basic properties on some rudimentary modules that are treated as black box routines, then describe three core modules in detail, and finally combine these procedures in the adaptive algorithm TAFEM.

4.1. Black Box Modules.

As in [KMSS12], we use standard modules `ADAPT_INIT`, `COARSEN`, `MARK_REFINE`, and `SOLVE` as black box routines. In particular, we use the subroutine `MARK_REFINE` in an object-oriented fashion, i. e., the functionality of `MARK_REFINE` changes according to its arguments. We next state the basic properties of these routines.

Assumption 12 (Properties of modules)**.** *We suppose that all rudimentary modules terminate with an output having the following properties.*

(1) For a given initial datum $u_0 \in L^2(\Omega)$ and tolerance $\texttt{TOL}_0 > 0$, the output

$$(U_0, \mathcal{G}_0) = \texttt{ADAPT_INIT}(u_0, \mathcal{G}_{init}, \texttt{TOL}_0)$$

is a refinement $\mathcal{G}_0 \geqslant \mathcal{G}_{init}$ and an approximation $U_0 \in \mathbb{V}(\mathcal{G}_0)$ to u_0 such that $\mathcal{E}_0^2(u_0, \mathcal{G}_0) \leqslant \texttt{TOL}_0^2$.

(2) For given $g \in L^2(\Omega)$, $\bar{f} \in \mathbb{P}_s(L^2(\Omega))$, $t_\star \in (0,T)$, $I = (t_\star, t_\star + \tau] \subset (t_\star, T]$, and $\mathcal{G} \in \mathbb{G}$, the output

$$U_I = \texttt{SOLVE}(g, \bar{f}, t, \tau, \mathcal{G})$$

is the solution $U_I \in \mathbb{P}_s(I, \mathbb{V}(\mathcal{G}))$ to the discrete elliptic problem

$$\int_I \langle \partial_t U_I, V\rangle_\Omega + \mathcal{B}[U_I, V]\,\mathrm{d}t + \langle U_I(t), V(t)\rangle_\Omega = \langle g, V\rangle_\Omega + \int_I \langle \bar{f}, V\rangle_\Omega \,\mathrm{d}t$$

for all $V \in \mathbb{P}_s(\mathbb{V}(\mathcal{G}))$; compare with (2.3). Hereby we assume exact integration and linear algebra.

(3) For a given grid $\mathcal{G} \in \mathbb{G}$ and a discrete function $V \in \mathbb{V}(\mathcal{G})$ the output

$$\mathcal{G}_* = \texttt{COARSEN}(V, \mathcal{G})$$

satisfies $\mathcal{G}_* \leqslant \mathcal{G}$.

(4) For a given grid $\mathcal{G}$ and a set of indicators $\{\mathcal{E}_E\}_{E\in\mathcal{G}}$ the output

$$\mathcal{G}_* = \texttt{MARK_REFINE}(\{\mathcal{E}_E\}_{E\in\mathcal{G}}, \mathcal{G}) \in \mathbb{G}$$

is a conforming refinement of $\mathcal{G}$, where at least one element in the subset $\operatorname{argmax}\{\mathcal{E}_E : E \in \mathcal{G}\} \subset \mathcal{G}$ has been refined.

(5) For given grids $\mathcal{G}, \mathcal{G}_{old} \in \mathbb{G}$ and a set of indicators $\{\mathcal{E}_E\}_{E\in\mathcal{G}}$, the output

$$\mathcal{G}_* = \textit{MARK_REFINE}(\{\mathcal{E}_E\}_{E\in\mathcal{G}}, \mathcal{G}, \mathcal{G}_{old}) \in \mathbb{G}$$

is a conforming refinement of $\mathcal{G}$, where at least one element of the set $\{E \in \mathcal{G} : h_{\mathcal{G}|E} > h_{\mathcal{G}_{old}|E}\}$ of coarsened elements (with respect to $\mathcal{G}_{\rm old}$) *is refined.*

For a more detailed description of these modules see Section 3.3.1 of [KMSS12].

4.2. **The Core Modules.** The first core module `CONSISTENCY` controls the consistency error $\mathcal{E}_f$. Recalling its definition in (3.7b), we see that the consistency error is solely influenced by the time-step size and can be computed without solving expensive discrete systems. Therefore, `CONSISTENCY` is used in the initialization of each time step to adjust the time-step-size such that the local consistency indicator $\mathcal{E}_f^2(f,t,\tau)$ is below a local tolerance $\texttt{tol}_f$. It is important to notice that this module follows the classic *thresholding* algorithm, which ensures quasi-optimal order of convergence in terms of the degrees of freedom; compare e.g. with [BDDP02].

Algorithm 1 Module `CONSISTENCY` (Parameters $\sigma, \kappa_1 \in (0,1)$ and $\kappa_2 > 1$)

`CONSISTENCY`$(f, t, \tau, \texttt{tol}_f)$

1: compute $\mathcal{E}_f^2(f,t,\tau)$
2: **while** $\mathcal{E}_f^2(f,t,\tau) < \sigma\,\texttt{tol}_f^2$ and $\tau < T - t$ **do** ★ enlarge τ
3: $\quad\tau = \min\{\kappa_2\tau, T-t\}$
4: $\quad$compute $\mathcal{E}_f^2(f,t,\tau)$
5: **end while**
6: **while** $\mathcal{E}_f^2(f,t,\tau) > \texttt{tol}_f^2$ **do** ★ reduce τ
7: $\quad\tau = \kappa_1\tau$
8: $\quad$compute $\mathcal{E}_f^2(f,t,\tau)$
9: **end while**
10: $\bar{f} = f_{[t,t+\tau]}$
11: **return** $\bar{f}, \tau$

We start with termination of the module `CONSISTENCY`.

Lemma 13 (Termination of `CONSISTENCY`)**.** *Assume $f \in L^2((0,T);L^2(\Omega))$. Then for any $t \in (0,T)$ and $\tau^{in} \in (0, T-t]$,*

$$(\bar{f}, \tau) = \textit{CONSISTENCY}(f, t, \tau^{in}, \texttt{tol}_f)$$

terminates and

$$\mathcal{E}_f^2(f,t,\tau) \leqslant \texttt{tol}_f^2. \tag{4.1}$$

Proof. The proof is straightforward since $\mathcal{E}_f^2(f,t,\tau)$ is monotone non-increasing and $\mathcal{E}_f^2(f,t,\tau) \to 0$ when $\tau \to 0$. □

Obviously, a local control of the form (4.1) does not guarantee, that the global consistency error is below some prescribed tolerance $\texttt{TOL}_f$. For this reason, we first precompute some local tolerance $\texttt{tol}_f$ from the global tolerance $\texttt{TOL}_f$ by the following module `TOLFIND`.

Algorithm 2 TOLFIND(Parameters: $\tilde{\tau}_0$)

TOLFIND$(f, T, \mathtt{TOL}_f)$

1: initialize N_f and set $\mathtt{tol}_f = \mathtt{TOL}_f$, $\tilde{t}_0 = 0$,
2: **loop forever**
3: $\quad\epsilon = n = 0$
4: $\quad$**do**
5: $\quad\quad n = n + 1$
6: $\quad\quad (f_n, \tilde{\tau}_n) =$ CONSISTENCY$(f, \tilde{t}_{n-1}, \tilde{\tau}_{n-1}, \mathtt{tol}_f)$
7: $\quad\quad \epsilon = \epsilon + \mathcal{E}_f^2(f, \tilde{t}_{n-1}, \tilde{\tau}_n)$
8: $\quad$**while** $\tilde{t}_n = \tilde{t}_{n-1} + \tilde{\tau}_n < T$
9: $\quad N_f = n$
10: $\quad$**if** $\epsilon > \frac{1}{2}\mathtt{TOL}_f^2$ **then**
11: $\quad\quad \mathtt{tol}_f^2 = \frac{1}{2}\mathtt{tol}_f^2$
12: $\quad$**else**
13: $\quad\quad$**break** ★ std. exit
14: $\quad$**end if**
15: **end loop forever**
16: $\mathtt{tol}_f^2 = \min\{\mathtt{tol}_f^2,\ \frac{\mathtt{TOL}_f^2}{2N_f}\}$
17: **return** $\mathtt{tol}_f$

The next result states that if all local consistency indicators are below the threshold $\mathtt{tol}_f$ then the accumulation of the consistency indicators stays indeed below the prescribed global tolerance $\mathtt{TOL}_f$.

Lemma 14 (Termination of TOLFIND)**.** *Assume $f \in L^2((0,T); L^2(\Omega))$. Then for any $\mathtt{TOL}_f > 0$, we have that*

$$\mathtt{tol}_f = \mathtt{TOLFIND}(f, T, \mathtt{TOL}_f) > 0$$

terminates. Moreover, let $0 = t_0 < t_1 < \cdots < t_N = T$ be arbitrary with $\tau_n = t_n - t_{n-1}$, $n = 1, \dots, N$, then

$$\mathcal{E}_f^2(f, t_{n-1}, \tau_n) \leqslant \mathtt{tol}_f^2,\ n = 1, \dots, N \quad \Rightarrow \quad \sum_{n=1}^{N} \mathcal{E}_f^2(f, t_{n-1}, \tau_n) \leqslant \mathtt{TOL}_f^2. \tag{4.2}$$

Proof. The proof is divided into three steps.

1 We show that the process from lines 4 to 8 terminates. To this end, we recall the parameters $\sigma, \kappa_1 \in (0,1)$ and $\kappa_2 > 1$ from CONSISTENCY$(f, \tilde{t}_{n-1}, \tilde{\tau}_{n-1}, \mathtt{tol}_f)$. We argue by contradiction and assume that an infinite monotone sequence $\{\tilde{t}_n\}_{n\geqslant 0} \subset [0,T]$ is constructed by TOLFIND with $\lim_{n\to\infty} \tilde{t}_n = t^\star \in (0,T]$.

Let us first assume that $t^\star < T$, and let $\ell_0, m_0 \in \mathbb{N}$ such that $\kappa_2^{\ell_0} \geqslant \kappa_1^{-m_0} \geqslant \kappa_2$. Then there exists $n_0 \in \mathbb{N}$, such that

$$t^\star + \kappa_2^{\ell_0}\tilde{\tau}_n < T \qquad \text{and} \qquad \mathcal{E}_f^2(f, \tilde{t}_n, \kappa_2^{\ell_0 - 1}\tilde{\tau}_n) \leqslant \sigma\mathtt{tol}_f^2 \tag{4.3}$$

for all $n \geqslant n_0$ since $\tilde{\tau}_n \to 0$ and

$$\mathcal{E}_f^2(f, \tilde{t}_n, \kappa_2^{\ell_0-1}\tilde{\tau}_n) \leqslant \|f\|^2_{\Omega\times(\tilde{t}_n, \tilde{t}_n + \kappa_2^{\ell_0-1}\tilde{\tau}_n)} \to 0 \quad \text{as } n \to \infty.$$

Therefore, from the loops in lines 2 to 5 and in 6 to 9 of CONSISTENCY, we conclude that $\tilde{\tau}_{n_0+1} \geqslant \kappa_2^{\ell_0}\kappa_1^{m_0}\tilde{\tau}_{n_0} \geqslant \tilde{\tau}_{n_0}$. Indeed, we have by (4.3) and

$$\mathcal{E}_f^2(f, \tilde{t}_{n_0}, \kappa_2^{\ell}\kappa_1^{m_0}\tilde{\tau}_{n_0}) \leqslant \mathcal{E}_f^2(f, \tilde{t}_{n_0}, \kappa_2^{\ell-1}\tilde{\tau}_{n_0}) \leqslant \sigma\mathtt{tol}_f^2$$

that $\ell \geqslant \ell_0$ and $m \leqslant m_0$. Consequently, we have $\tilde{\tau}_n \geqslant \tilde{\tau}_{n_0}$, for all $n \geqslant n_0$ by induction. This is the contradiction.

Let now $t^\star = T$, then with similar arguments as before, we conclude that $\mathcal{E}_f^2(f, \tilde{t}_n, T - \tilde{t}_n) \leqslant \sigma \mathtt{tol}_f^2$ for some $n \in \mathbb{N}$, and we have from line 3 of `CONSISTENCY`, that $\tilde{\tau}_n = T - \tilde{t}_n$, which contradicts the assumption in this case.

2 We next check that the condition of line 10 is violated after finite many steps. Since the span of characteristics of dyadic intervals is dense in $L^2(0,T)$, we can choose $M > 0$, such that the squared consistency error on the grid of 2^M uniform intervals is below $\frac{1}{4}\mathtt{TOL}_f^2$. We split the intervals generated in $\mathtt{TOLFIND}(f, T, \mathtt{tol}_f)$ into

$$\mathbb{I}_{in} := \big\{n : (\tilde{t}_{n-1}, \tilde{t}_n] \subset T(m2^{-M}, (m+1)2^{-M}] \text{ for some } m \in \{0, \dots, 2^M - 1\}\big\}$$

and $\mathbb{I}_{out} := \{1, \dots, N_f\} \backslash \mathbb{I}_{in}$ according to whether or not they are included in one of the dyadic intervals. Therefore, we have, with the monotonicity of the consistency error and $\#\mathbb{I}_{out} \leqslant 2^M$, that

$$\epsilon = \sum_{n \in \mathbb{I}_{in}} \mathcal{E}_f^2(f, \tilde{t}_{n-1}, \tilde{\tau}_n) + \sum_{n \in \mathbb{I}_{out}} \mathcal{E}_f^2(f, \tilde{t}_{n-1}, \tilde{\tau}_n) \leqslant \frac{1}{4}\mathtt{TOL}_f^2 + 2^M \mathtt{tol}_f^2.$$

Taking $\mathtt{tol}_f^2 < 2^{-(M+2)}\mathtt{TOL}_f^2$, we see that the condition of line 10 is violated, which proves the assertion.

3 Combining the above steps, we conclude that `TOLFIND` terminates and it remains to prove (4.2). To this end, we proceed similarly as in 2 and let

$$\mathbb{I}_{in} := \big\{n : (t_{n-1}, t_n] \subset (\tilde{t}_{m-1}, \tilde{t}_m] \text{ for some } m \in \{1, \dots, N_f\}\big\}.$$

and $\mathbb{I}_{out} := \{1, \dots, N\} \backslash \mathbb{I}_{in}$. By monotonicity, we have $\sum_{n \in \mathbb{I}_{in}} \mathcal{E}_f^2(f, t_{n-1}, \tau_n) \leqslant \sum_{n=1}^{N_f} \mathcal{E}_f^2(f, \tilde{t}_{n-1}, \tilde{\tau}_n) \leqslant \mathtt{TOL}_f^2/2$ and thus the assertion follows from

$$\begin{aligned}\sum_{n=1}^{N} \mathcal{E}_f^2(f, t_{n-1}, \tau_n) &= \sum_{n \in \mathbb{I}_{in}} \mathcal{E}_f^2(f, t_{n-1}, \tau_n) + \sum_{n \in \mathbb{I}_{out}} \mathcal{E}_f^2(f, t_{n-1}, \tau_n) \\ &\leqslant \frac{\mathtt{TOL}_f^2}{2} + N_f \mathtt{tol}_f^2 = \frac{\mathtt{TOL}_f^2}{2} + N_f \frac{\mathtt{TOL}_f^2}{2N_f} \leqslant \mathtt{TOL}_f^2. \qquad \square\end{aligned}$$

Remark 15 (Estimation of $\mathtt{tol}_f$ under regularity assumptions)**.** *Supposing the regularity assumption $f \in H^s((0,T); L^2(\Omega))$, $s \in (0,1]$, the following idea may be used as an alternative for the estimation of $\mathtt{tol}_f$ with `TOLFIND`.*

Let $\delta > 0$. Then using Lemma 13 together with Poincaré's inequality in H^s and the fact that there are at most $\frac{T}{\delta}$ disjoint intervals of length δ in $(0,T]$, we obtain

$$\begin{aligned}\sum_{n=1}^{N} \mathcal{E}_f^2(f, t_{n-1}, \tau_n) &= \sum_{\tau_n > \delta} \mathcal{E}_f^2(f, t_{n-1}, \tau_n) + \sum_{\tau_n \leqslant \delta} \mathcal{E}_f^2(f, t_{n-1}, \tau_n) \\ &\leqslant \frac{T}{\delta}\mathtt{tol}_f^2 + \sum_{\tau_n \leqslant \delta} \tau_n^{2s} \|f\|^2_{H^s(t_{n-1}, t_n, L^2(\Omega))} \\ &= \frac{T}{\delta}\mathtt{tol}_f^2 + \delta^{2s}\|f\|^2_{H^s(0,T,L^2(\Omega))}.\end{aligned}$$

By choosing $\delta = \left(\frac{T\,\mathtt{tol}_f}{\|f\|_{H^s(0,T,L^2(\Omega))}}\right)^{\frac{2}{2s+1}}$, the previous estimate turns into

$$\sum_{n=1}^{N} \mathcal{E}_f^2(f, t_{n-1}, \tau_n) \leqslant 2\,T^{\frac{2s}{2s+1}}\,\|f\|^{\frac{2}{2s+1}}_{H^s(0,T,L^2(\Omega))}\,\mathtt{tol}_f^{\frac{4s}{2s+1}}.$$

In other words, if a priori knowledge on the regularity of the right hand side is available then `TOLFIND` *can be replaced by the somewhat simpler term*

$$\mathtt{tol}_f^2 = 2^{-\frac{2s+1}{2s}}\, T^{-1} \|f\|_{H^s(0,T,L^2(\Omega))}^{-\frac{1}{s}}\, \mathtt{TOL}_f^{\frac{2s+1}{s}}.$$

We turn to the module `ST_ADAPTATION`, listed in Algorithm 3, which handles a single time-step. The module adapts the grid and the time-step-size according to the indicators involving the discrete solution of the current time-step, namely the space indicator $\mathcal{E}_{\mathcal{G}}$ and the separated coarsening and time indicators $\mathcal{E}_c$ and $\mathcal{E}_\tau$. The routine requires right at te start of each iteration the computation of the discrete solution on the actual grid and with the current time-step-size; see line 5. Note that in `ST_ADAPTATION` only refinements are performed (both in space and in time). Recalling the discussion in the introductory section, Section 1, we aim to use a thresholding algorithm for the indicators $\mathcal{E}_\tau$, in order to equally distribute the time error. To this end, we first need to guarantee $\mathcal{E}_* \leqslant 0$ in order to control the global time error with the help of the uniform energy estimate form Corollary 11. Since for neither the space nor the coarsening errors there is a similar control available, we relate the corresponding indicators to the time or the consistency indicator, i.e. to adapt the spatial triangulation until

$$\mathcal{E}_c^2, \mathcal{E}_{\mathcal{G}}^2 \leqslant \mathcal{E}_\tau^2 + \mathcal{E}_f^2. \tag{4.4}$$

Here we have invoked the consistency indicator $\mathcal{E}_f$ on the right hand side although it is controlled by `CONSISTENCY` outside `ST_ADAPTATION` – note that $\mathcal{E}_f$ does not depend on the discrete solution. In fact, from the uniform energy estimate, Corollary 11, we have that $\mathcal{E}_\tau$ vanishes faster than $\mathcal{E}_f$ by one order, when no additional regularity of f is assumed. Consequently, the time-step size is dictated by $\mathcal{E}_f$, which may leed to $\mathcal{E}_\tau \ll \mathtt{tol}_{\mathcal{G}\tau}$. Thanks to Lemma 14, we expect that (4.4) leads to an equal distribution of the errors in time in most cases. However, the case $\max\{\mathcal{E}_\tau, \mathcal{E}_f\} \ll \min\{\mathtt{tol}_{\mathcal{G}\tau}, \mathtt{tol}_f\}$ cannot be avoided theoretically, hence we have accomplished (4.4) with a safeguard L^∞ marking; compare with lines 11 and 13 of `ST_ADAPTATION`.

Note that in the above discussion, we have concentrated on an equal distribution in time and have tacitly assumed that in each time-step the local space indicators are optimally distributed, which is motivated by the optimal convergence analysis for elliptic problems; compare e.g. with [Ste07, CKNS08, DKS16].

Remark 16. *We note that the* ***if*** *conditions in lines 11 and 13 of* `ST_ADAPTATION` *may involve additional parameters. For instance, line 13 may be replaced by*

15: ***else if*** $\mathcal{E}_c^2(U_t^-, \tau, \mathcal{G}) \geqslant \gamma_c\, \mathcal{E}_\tau^2(U_t^+, U_t^-, \tau, \mathcal{G}) + \rho_c \mathcal{E}_f^2(f, t, \tau) + \sigma_c \tau\, \mathtt{tol}_{\mathcal{G}\tau}$ ***then***

with $\gamma_c, \rho_c, \sigma_c > 0$ *and similar for the space indicator* $\mathcal{E}_{\mathcal{G}}$ *in line 11 with constants* $\gamma_{\mathcal{G}}, \rho_{\mathcal{G}}, \sigma_{\mathcal{G}} > 0$. *This requires some modifications of the TAFEM, which would make the presentation more technical. For the sake of clarity of the presentation, we decided to skip these customisation possibilities; compare also with Remark 21.*

4.3. **The main module TAFEM.** We are now in the position to formulate the TAFEM in Algorithm 4 below.

In the initialization phase the given tolerance $\mathtt{TOL} > 0$ is split into tolerances $\mathtt{TOL}_0, \mathtt{TOL}_f, \mathtt{TOL}_{\mathcal{G}\tau} > 0$. Next, `ADAPT_INIT` provides a sufficiently good approximation U_0 of the initial datum u_0. Then the time-step iteration is entered, where each single time-step consists of the following main steps. We first initialize the time-step size by `CONSISTENCY` and then conduct one coarsening step with `COARSEN`. The adaptation of the grid and time-step-size with respect to the indicators for the spatial, temporal, and coarsening error is done by `ST_ADAPTATION`.

Algorithm 3 Module ST_ADAPTATION (Parameter $\kappa \in (0,1)$)

ST_ADAPTATION$(U_t^-, f, t, \tau, \mathcal{G}, \mathcal{G}_{\text{old}}, \texttt{tol}_{\mathcal{G}_\tau})$

compute $\mathcal{E}_f^2(f,t,\tau)$
loop forever
  $I = [t, t+\tau]$
  $\bar{f} = f_I$
  $U_I = \texttt{SOLVE}(U_t^-, \bar{f}, t, \tau, \mathcal{G})$
  $U_t^+ = \lim_{s \searrow t} U_I(s)$
  compute $\{\mathcal{E}_{\mathcal{G}}^2(U_I, U_t^-, t, \tau, \bar{f}, \mathcal{G}, E)\}_{E\in\mathcal{G}}$, $\{\mathcal{E}_*^2(U_t^+, U_t^-, \tau, \mathcal{G}, E)\}_{E\in\mathcal{G}}$
  $\mathcal{E}_\tau^2(U_t^+, U_t^-, \tau, \mathcal{G})$, and $\{\mathcal{E}_c^2(U_t^-, \tau, \mathcal{G}, E)\}_{E\in\mathcal{G}}$
  if $\mathcal{E}_\tau^2(U_t^+, U_t^-, \tau, \mathcal{G}) > \texttt{tol}_{\mathcal{G}_\tau}^2$ **then**
    $\tau = \kappa\tau$ A
    compute $\mathcal{E}_f^2(f,t,\tau)$
  else if $\mathcal{E}_{\mathcal{G}}^2(U_I, U_t^-, t, \tau, \bar{f}, \mathcal{G}) > \mathcal{E}_\tau^2(U_t^+, U_t^-, \tau, \mathcal{G}) + \mathcal{E}_f^2(f,t,\tau) + \tau\texttt{tol}_{\mathcal{G}_\tau}$ **then**
    $\mathcal{G} = \texttt{MARK_REFINE}(\{\mathcal{E}_{\mathcal{G}}^2(U_I, U_t^-, t, \tau, \bar{f}, \mathcal{G}, E)\}_{E\in\mathcal{G}}, \mathcal{G})$ B
  else if $\mathcal{E}_c^2(U_t^-, \tau, \mathcal{G}) > \mathcal{E}_\tau^2(U_t^+, U_t^-, \tau, \mathcal{G}) + \mathcal{E}_f^2(f,t,\tau) + \tau\texttt{tol}_{\mathcal{G}_\tau}$ **then**
    $\mathcal{G} = \texttt{MARK_REFINE}(\{\mathcal{E}_c^2(U_t^-, \tau, \mathcal{G}, E)\}_{E\in\mathcal{G}}, \mathcal{G})$ C
  else if $\mathcal{E}_*^2(U_t^+, U_t^-, \tau, \mathcal{G}) > 0$ **then**
    $\mathcal{G} = \texttt{MARK_REFINE}(\{\mathcal{E}_*^2(U_t^+, U_t^-, \tau, \mathcal{G}, E)\}_{E\in\mathcal{G}}, \mathcal{G}, \mathcal{G}_{\text{old}})$ D
  else
    break ★exit
  end if
end loop forever
return $U_I, \tau, \bar{f}, \mathcal{G}$

Algorithm 4 TAFEM

initialize $\mathcal{G}_{\text{init}}$, τ_0 and set $t_0 = 0$, $n = 0$
split tolerance $\texttt{TOL} > 0$ such that $\texttt{TOL}_0^2 + 3\,\texttt{TOL}_f^2 + \texttt{TOL}_{\mathcal{G}_\tau}^2 = \texttt{TOL}^2$
$\texttt{tol}_f = \texttt{TOLFIND}(f, T, \texttt{TOL}_f)$
$(U_0^-, \mathcal{G}_0) = \texttt{ADAPT_INIT}(u_0, \mathcal{G}_{\text{init}}, \texttt{TOL}_0)$
compute $C_T := 6\sqrt{6\,C_{c\tau}\,T}\left(\|f\|_{\Omega\times(0,T)}^2 + \left\|\!\left|U_0^-\right|\!\right\|_\Omega^2\right)^{\frac{1}{2}} + 2\,T$
do
  $n = n + 1$
  $\tau_n = \min\{\tau_{n-1}, T - t\}$
  $\tau_n = \texttt{CONSISTENCY}(f, t_{n-1}, \tau_{n-1}, \texttt{tol}_f)$
  $\mathcal{G}_n = \texttt{COARSEN}(U_{n-1}^-, \mathcal{G}_{n-1})$
  $(U_{|I_n}, \tau_n, f_n, \mathcal{G}_n) = \texttt{ST_ADAPTATION}(U_{n-1}^-, t_n, \tau_n, f, \mathcal{G}_n, \mathcal{G}_{n-1}, \texttt{TOL}_{\mathcal{G}_\tau}^2/C_T)$
  $U_n^- = U_{|I_n}(t_{n-1} + \tau_n)$
while $t_n = t_{n-1} + \tau_n < T$

5. Convergence

In this section, we first prove that the core modules and TAFEM terminate and then verify that the estimators and thus the error is below the given tolerance. Throughout the section we suppose that the black-box modules satisfy Assumption 12.

Before turning to the main module ST_ADAPTATION, as an auxiliary result, we shall consider convergence of the adaptive finite element method for stationary elliptic problems of the kind (3.11), which have to be solved in each timestep.

Algorithm 5 AFEM

AFEM$(v^-, \bar{f}, t, \tau, \mathcal{G}^0)$
1: set $k = 0$
2: **loop forever**
3: $U_\tau^k = \texttt{SOLVE}(v^-, \bar{f}, 0, \tau, \mathcal{G}^k)$
4: compute $\{\mathcal{E}^2_{\mathcal{G}}(U_\tau^k, v^-, 0, \tau, \bar{f}, \mathcal{G}, E)\}_{E\in\mathcal{G}}$,
5: $\mathcal{G}^{k+1} = \texttt{MARK_REFINE}(\{\mathcal{E}^2_{\mathcal{G}}(U_\tau^k, v^-, 0, \tau, \bar{f}, \mathcal{G}^k, E)\}_{E\in\mathcal{G}}, \mathcal{G}^k)$
6: $k = k + 1$
7: **end loop forever**

Proposition 17 (Convergence for the Elliptic Problem)**.** *Suppose that $U_t^- \in L^2(\Omega)$, $\bar{f} \in \mathbb{P}_s(L^2(\Omega))$, and $\tau > 0$. Then, starting from any grid $\mathcal{G}^0 \in \mathbb{G}$ we have for the sequence $\{\mathcal{G}^k, U_\tau^k\}_{k\geqslant 0} \subset \mathbb{G} \times \mathbb{P}_s(\mathbb{V})$ generated by* AFEM$(v^-, \bar{f}, t, \tau, \mathcal{G}^0)$*, that*

$$\mathcal{E}^2_{\mathcal{G}}(U_\tau^k, v^-, \tau, t, \bar{f}, \mathcal{G}^K) \to 0 \quad \text{as } k \to \infty.$$

Proof. Recalling Remark 9, we have that $\mathcal{E}^2_{\mathcal{G}}(U_\tau^k, v^-, \tau, 0, \bar{f}, \mathcal{G}^K)$ are the standard residual based a posteriori error estimators for the coercive problem (3.11). From Lemmas 4 and 5 and Assumption 12 on MARK_REFINE, we have that the conditions of [Sie11, Theorem 2.2] are satisfied. This yields the assertion. □

Lemma 18 (Termination of ST_ADAPTATION)**.** *For any $t \in (0, T)$, $\tau^{in} \in (0, T - t]$, $\mathcal{G}, \mathcal{G}_{old} \in \mathbb{G}$, and $U_t^- \in \mathbb{V}(\mathcal{G}_{old})$, we have that*

$$(U_I, \tau, \bar{f}, \mathcal{G}) = \textit{ST_ADAPTATION}(U_t^-, f, t, \tau^{in}, \mathcal{G}_{in}, \mathcal{G}_{old}, \mathtt{tol}_{\mathcal{G}\tau})$$

terminates. Moreover, we have $\mathcal{G} \geqslant \mathcal{G}_0$, $\mathcal{E}^2_*(U_t^+, U_t^-, \tau, \mathcal{G}) \leqslant 0$,

$$\tau^{in} \geqslant \tau \geqslant \min\left\{\tau^{in}, \frac{\kappa\, \mathtt{tol}^2_{\mathcal{G}\tau}}{6\big(\|f\|^2_{\Omega\times(t,t+\tau)} + \big\|U_t^-\big\|^2_\Omega\big)}\right\},$$

and the indicators satisfy the tolerances

$$\begin{aligned}
\mathcal{E}^2_\tau(U_t^+, U_t^-, \tau, \mathcal{G}) &\leqslant \mathtt{tol}^2_{\mathcal{G}\tau},\\
\mathcal{E}^2_{\mathcal{G}}(U_I, U_t^-, t, \tau, \bar{f}, \mathcal{G}) &\leqslant \mathcal{E}^2_\tau(U_t^+, U_t^-, \tau, \mathcal{G}) + \mathcal{E}^2_f(f, t, \tau) + \tau\,\mathtt{tol}_{\mathcal{G}\tau},\\
\mathcal{E}^2_c(U_t^-, \tau, \mathcal{G}) &\leqslant \mathcal{E}^2_\tau(U_t^+, U_t^-, \tau, \mathcal{G}) + \mathcal{E}^2_f(f, t, \tau) + \tau\,\mathtt{tol}_{\mathcal{G}\tau},
\end{aligned}$$

where $U_t^+ = \lim_{s\searrow t} U_{(t,t+\tau]}(s)$.

Proof. In each iteration of the loop in ST_ADAPTATION at first, a discrete solution U_I is computed on the current grid $\mathcal{G}$ with the actual time-step size τ. Then either the time-step-size is reduced or the actual grid is refined. More precisely, exactly one of the statements labeled as A,..., D in Algorithm 3 is executed, any of them terminating by Assumption 12. Whenever one of these statements is executed the corresponding indicator is positive.

In statement C the grid is refined due to the coarsening indicator $\mathcal{E}_c$. Thanks to Assumption 12 (5), after a finite number of executions of C, a grid $\mathcal{G}$ is obtained

with $\mathcal{G}_{\text{old}} \leqslant \mathcal{G}$ and thus $\mathcal{E}_c^2(U_t^-, \mathcal{G}) = 0$, i.e. statement $\boxed{\mathsf{C}}$ is not entered anymore. This happens irrespective of refinements in other statements.

In statement $\boxed{\mathsf{D}}$ the grid is refined with respect to the indicators $\mathcal{E}_*$ controlling the energy gain due to coarsening. Therefore, it follows from the same reasoning as for statement $\boxed{\mathsf{C}}$, that statement $\boxed{\mathsf{D}}$ is also executed at most until the coarsening is fully removed after finite many refinement steps.

It is important to notice that if statement $\boxed{\mathsf{A}}$ is executed then the conditions in lines 15 and 8 imply

$$\frac{1}{\tau} \leqslant \frac{1}{\tau} 6\,\tau \left\| U_t^+ - \Pi_{\mathcal{G}} U_t^- \right\|_\Omega^2 \frac{1}{\mathtt{tol}_{\mathcal{G}\tau}^2} \leqslant \frac{1}{\mathtt{tol}_{\mathcal{G}\tau}^2} 6 \left(\|f\|_{\Omega\times(t,t+\tau)}^2 + \left\| U_t^- \right\|_\Omega^2 \right),$$

where the last inequality follows from Corollary 11. This implies that τ is bounded from below and thus Statement $\boxed{\mathsf{A}}$ is only executed finite many times. This also proves the asserted lower bound on the final time-step size.

Assuming that `ST_ADAPTATION` does not terminate, we infer from the fact that all other statements are only conducted finitely many times, that statement $\boxed{\mathsf{B}}$ has to be executed infinite many times. In other words, the loop reduces to the adaptive iteration `AFEM` with fixed data U_t^-, $\bar{f}$, t, and τ. Therefore, Proposition 17 contradicts the condition in line 11.

In summary, we deduce that `ST_ADAPTATION` terminates and the iteration is abandoned in line 18. This proves the assertion. □

We next address the termination of the main module TAFEM.

Proposition 19 (Termination of TAFEM)**.** *The adaptive algorithm TAFEM terminates for any initial time-step-size $\tau_0 > 0$ and produces a finite number of time instances $0 = t_0 < \cdots < t_N = T$.*

Moreover, we have $\mathcal{E}_0^2(u_0, \mathcal{G}_0) \leqslant \mathtt{TOL}_0^2$ and that the consistency error complies with (4.2). For all $n = 1, \dots, N$, we have that the estimates in Lemma 18 are satisfied with $t = t_{n-1}$, $\tau = \tau_n$, $U_I = U_{|I_n}$, $U_t^\pm = U_{n-1}^\pm$, $\mathcal{G} = \mathcal{G}_n$, and $\mathcal{G}_{old} = \mathcal{G}_{n-1}$.

Proof. Each loop starts with setting the time-step-size such that $\tau_n \leqslant T - t_n$, $n \in \mathbb{N}$. Thanks to Assumption 12 for the black-box modules, Lemma 13 for `CONSISTENCY`, and Lemma 18 for `ST_ADAPTATION`, all modules of TAFEM terminate and in each timestep the asserted properties are satisfied.

Since we have $\mathcal{E}_*^2(U_{n-1}^+, U_{n-1}^-, \tau_n, \mathcal{G}_n) \leqslant 0$ for all n, we may conclude $\left\| U_{n-1}^- \right\|_\Omega \leqslant \|f\|_{\Omega\times(0,T)}^2 + \|U_0\|_\Omega$ from Lemma 11 and thus it follows with Lemma 18, that

$$\tau_n^{\text{in}} \geqslant \tau_n \geqslant \min\left\{ \tau_n^{\text{in}}, \frac{\kappa\, \mathtt{tol}_{\mathcal{G}\tau}^2}{12\big(\|f\|_{\Omega\times(0,T)}^2 + \|U_0\|_\Omega^2\big)} \right\},$$

where $\tau_n^{\text{in}} = \mathtt{CONSISTENCY}(f, t_{n-1}, \tau_{n-1}, \mathtt{tol}_f)$. Assuming that the final time is not reached implies $\tau_n \to 0$ as $n \to \infty$ and therefore there exists $n_0 \in \mathbb{N}$, such that $\tau_n = \tau_n^{\text{in}}$ for all $n \geqslant n_0$. Now, the contradiction follows as in step $\boxed{1}$ of the proof of Lemma 14. □

Collecting the results derived above allows us to prove the main result.

Theorem 20 (Convergence into Tolerance)**.** *Algorithm TAFEM computes for any prescribed tolerance $\mathtt{TOL} > 0$ and initial time-step-size $\tau_0 > 0$ a partition $0 < t_0 < \cdots < t_N = T$ with associated meshes $\{\mathcal{G}_n\}_{n=0,\dots,N}$, such that we have for the corresponding approximation $\mathcal{U} \in \mathbb{W}(0,T)$ from (2.8), that*

$$\|u - \mathcal{U}\|_{\mathbb{W}(0,T)} \leqslant \mathtt{TOL}.$$

Proof. Thanks to Proposition 19, we have that TAFEM terminates and it remains to prove the error bound. For the sake of brevity of the presentation, we shall use the abbreviations

$$\mathcal{E}_\tau^2(n) := \mathcal{E}_\tau^2(U_{n-1}^+, U_{n-1}^-, \tau_n, \mathcal{G}_n), \qquad \mathcal{E}_f^2(n) := \mathcal{E}_f^2(f, t_{n-1}, \tau_n),$$
$$\mathcal{E}_\mathcal{G}^2(n) := \mathcal{E}_\mathcal{G}^2(U, U_{n-1}^-, t_{n-1}, \tau_n, f_n, \mathcal{G}_n), \quad \text{and} \quad \mathcal{E}_c^2(n) := \mathcal{E}_c^2(U_{n-1}^-, \tau, \mathcal{G}_n).$$

The initial error satisfies $\mathcal{E}_0^2(u_0, \mathcal{G}_0) \leqslant \mathtt{TOL}_0^2$ by by Assumption 12. Thanks to the choice of the precomputed local tolerance $\mathtt{tol}_f$, we know from Lemma 14 that the consistency error is bounded by $\mathtt{TOL}_f$, i.e. we have (4.2).

When finalizing a time-step, we also have from Lemma 19 that

$$\mathcal{E}_\tau^2(n) \leqslant \mathtt{tol}_{\mathcal{G}\tau}^2 \qquad \text{and} \qquad \mathcal{E}_\mathcal{G}^2(n), \mathcal{E}_c^2(n) \leqslant \mathcal{E}_\tau^2(n) + \mathcal{E}_f^2(n) + \tau_n \mathtt{tol}_{\mathcal{G}\tau},$$

with $\mathtt{tol}_{\mathcal{G}\tau} = \mathtt{TOL}_{\mathcal{G}\tau}^2 / C_T$. Combining this with (3.14) and (4.2), we conclude

$$\begin{aligned}
\sum_{n=1}^N \mathcal{E}_\mathcal{G}^2(n) + \mathcal{E}_{c\tau}^2(U_{n-1}^+, U_{n-1}^-, \tau_n) &\leqslant \sum_{n=1}^N \mathcal{E}_\mathcal{G}^2(n) + \mathcal{E}_c^2(n) + \mathcal{E}_\tau^2(n) \\
&\leqslant \sum_{n=1}^N 2\,\tau_n \mathtt{tol}_{\mathcal{G}\tau} + 2\,\mathcal{E}_f^2(n) + 3\,\mathcal{E}_\tau^2(n) \\
&\leqslant 2\,T\,\mathtt{tol}_{\mathcal{G}\tau} + 2\,\mathtt{TOL}_f^2 + 3\sum_{n=1}^N \mathcal{E}_\tau^2(n).
\end{aligned}$$

Using Corollary 11 for the last term, we get for any $\delta > 0$, that

$$\begin{aligned}
\sum_{n=1}^N \mathcal{E}_\tau^2(n) &= \sum_{\tau_n > \delta} \mathcal{E}_\tau^2(n) + \sum_{\tau_n \leqslant \delta} \mathcal{E}_\tau^2(n) \\
&\leqslant \frac{T}{\delta} \mathtt{tol}_{\mathcal{G}\tau}^2 + \delta \sum_{n=1}^N 6\,C_\tau \left\| U_{n-1}^+ - \Pi_{\mathcal{G}_n} U_{n-1}^- \right\|_\Omega^2 \\
&\leqslant \frac{T}{\delta} \mathtt{tol}_{\mathcal{G}\tau}^2 + \delta 6\,C_\tau \left(\|f\|_{\Omega\times(0,T)}^2 + \|U_0\|_\Omega^2 \right)
\end{aligned}$$

and by choosing

$$\delta = \left(\frac{T}{6\,C_{c\tau} \left(\|f\|_{\Omega\times(0,T)}^2 + \|U_0\|_\Omega^2 \right)} \right)^{\frac{1}{2}} \mathtt{tol}_{\mathcal{G}\tau},$$

we obtain

$$\sum_{n=1}^N \mathcal{E}_\tau^2(n) \leqslant 2 \left(6\,C_{c\tau}\,T \left(\|f\|_{\Omega\times(0,T)}^2 + \|U_0\|_\Omega^2 \right) \right)^{\frac{1}{2}} \mathtt{tol}_{\mathcal{G}\tau}.$$

Inserting this into the above estimate yields

$$\begin{aligned}
&\sum_{n=1}^N \mathcal{E}_\mathcal{G}^2(n) + \mathcal{E}_{c\tau}^2(U_{n-1}^+, U_{n-1}^-, \tau_n) \\
&\qquad \leqslant \underbrace{\left(6\sqrt{6\,C_{c\tau}\,T} \left(\|f\|_{\Omega\times(0,T)}^2 + \|U_0\|_\Omega^2 \right)^{\frac{1}{2}} + 2\,T \right)}_{=C_T} \mathtt{tol}_{\mathcal{G}\tau} + 2\,\mathtt{TOL}_f^2 \\
&\qquad \leqslant \mathtt{TOL}_{\mathcal{G}\tau}^2 + 2\,\mathtt{TOL}_f^2.
\end{aligned}$$

Collecting the bounds for the indicators $\mathcal{E}_0$, $\mathcal{E}_\mathcal{G}$, $\mathcal{E}_{c\tau}$, and $\mathcal{E}_f$, recalling the splitting

$$\mathtt{TOL}_0^2 + 3\,\mathtt{TOL}_f^2 + \mathtt{TOL}_{\mathcal{G}\tau}^2 = \mathtt{TOL}^2,$$

and taking into account the upper bound of Proposition 6 proves the assertion. □

Remark 21. *In order to guarantee the main result (Theorem 20) also for the modifications of Remark 16 line 5 in TAFEM must be changed to*

5: compute $C_T := (1+\gamma_c+\gamma_{\mathcal{G}})\,2\sqrt{6\,C_{c\tau}\,T}\left(\|f\|^2_{\Omega\times(0,T)}+\left\|U_0^-\right\|^2_{\Omega}\right)^{\frac{1}{2}}+(\sigma_c+\sigma_{\mathcal{G}})\,T.$

Moreover, the splitting of the tolerances in line 2 must be changed to

2: split tolerance $\mathtt{TOL}>0$ *such that* $\mathtt{TOL}_0^2+(1+\rho_{\mathcal{G}}+\rho_c)\mathtt{TOL}_f^2+\mathtt{TOL}_{\mathcal{G}\tau}^2=\mathtt{TOL}^2$.

6. Numerical aspects and experiments

We conclude the article by illustrating some practical aspects of the implementation with three numerical experiments. We compare the presented algorithm TAFEM with the algorithm ASTFEM introduced in [KMSS12].

6.1. **The implementation.** The experiments are implemented in DUNE [BBD+16] using the DUNE-ACFEM (http://users.dune-project.org/projects/dune-acfem) module. The computations utilize linear conforming finite elements on space and dG(0) as time-stepping scheme. All simulations where performed on a Intel®Core™i7-6700HQ Processor with 64 GB RAM.

Both algorithms TAFEM and ASTFEM start from exactly the same initial mesh $\mathcal{G}_{\text{init}}$. The initial values are interpolated on the mesh and local refinements are performed in order to comply with the initial tolerance. On the resulting meshes the needed constants are computed (the minimal time-step size τ^* for ASTFEM and $\mathtt{tol}_f$ from `TOLFIND` for TAFEM).

In order to control $\mathcal{E}_c$ and $\mathcal{E}_*$, the algorithms need to handle two meshes and corresponding finite element spaces at every new time-step. This is realised exploiting the tree structure of the refinements of macro elements as in [KMSS12]. At every new time-step all elements on the mesh are marked to be coarsened up to two times and then adapted again if necessary. The mentioned estimators are computed only up to constants and used for the adaptive refinement progress. The spatial marking relies on the equi-distribution strategy, which marks every element with an estimator bigger than the arithmetic mean.

The following remark lists the tolerance splitting used by ASTFEM.

Remark 22. *In* [KMSS12]*, the ASTFEM uses the tolerance splitting*

$$\mathtt{TOL}^2 = \mathtt{TOL}_0^2 + T\widetilde{\mathtt{TOL}}_f^2 + T\widetilde{\mathtt{TOL}}_{\mathcal{G}\tau}^2 + \widetilde{\mathtt{TOL}}_*^2.$$

Thereby $\mathtt{TOL}_*^2$ *is used to compute a minimal safeguard step-size* τ_**. The method computes then an approximation* $\mathcal{U}\in\mathbb{W}(0,T)$ *to* (2.2)*, such that*

$$\mathcal{E}_0^2(u_0,\mathcal{G}_0)\leqslant\mathtt{TOL}_0^2,\qquad\sum_{n=1}^{N}\left\{\mathcal{E}_f^2(f,t_{n-1},\tau_n)\right\}\leqslant T\widetilde{\mathtt{TOL}}_f^2$$

and

$$\sum_{n=1}^{N}\left\{\mathcal{E}_{c\tau}^2(U_{n-1}^+,U_{n-1}^-,\tau_n)+\mathcal{E}_{\mathcal{G}}^2(U,U_{n-1}^-,t_n,\tau_n,f_n,\mathcal{G}_n)\right\}\leqslant T\widetilde{\mathtt{TOL}}_{\mathcal{G}\tau}^2+\widetilde{\mathtt{TOL}}_*^2.$$

This motivates the relation

$$T\widetilde{\mathtt{TOL}}_f^2=3\mathtt{TOL}_f^2,\quad\text{and}\quad T\widetilde{\mathtt{TOL}}_{\mathcal{G}\tau}^2+\widetilde{\mathtt{TOL}}_*^2=\mathtt{TOL}_{\mathcal{G}\tau}^2$$

in the examples below.

For the simulations presented below we have used the following comparable splittings for the two methods ASTFEM and TAFEM relative to the total tolerance $\mathtt{TOL}$*:*

- $\mathtt{TOL}_0^2=\frac{1}{10}\mathtt{TOL}^2$,
- $\mathtt{TOL}_f^2=T\widetilde{\mathtt{TOL}}_f^2=\frac{4}{10}\mathtt{TOL}^2$,
- $\mathtt{TOL}_{\mathcal{G}\tau}^2=T\widetilde{\mathtt{TOL}}_{\mathcal{G}\tau}^2+\widetilde{\mathtt{TOL}}_*^2=\frac{6}{10}\mathtt{TOL}^2$,

- $\widetilde{\mathtt{TOL}}_*^2 = \frac{1}{100}\mathtt{TOL}^2$.

6.2. **The experiments.** In this section, we introduce the three numerical experiments in detail and discuss the numerical results.

6.2.1. *Singularity in time.* This numerical experiment is constructed on the spatial domain $\Omega = (0,1)^2 \subset \mathbb{R}^2$ over the time interval $(0,T) = (0,2)$ with homogeneous Dirichlet boundary conditions and homogeneous initial data. The right-hand side f is choosen such that the exact solution is given by

$$u(\boldsymbol{x},t) = |t-\bar{t}|^\alpha \sin(\pi(x^2-x)t)\sin(\pi(y^2-y)t)$$

with parameters $\bar{t} = \frac{\pi}{3}$ and $\alpha = 0.7$. The graph of u has a singularity in time at $t = \frac{\pi}{3}$. Hence, the right-hand side contains the therm $\operatorname{sgn}(t-\bar{t})\alpha|t-\bar{t}|^{\alpha-1}$. A direct calculation shows that this term is L^2 -integrable but is not in H^1. This particular example shows one main advantage of TAFEM. In fact, in contrast to ASTFEM, TAFEM does not require the right hand side f to have temporal derivative in L^2 in order to control the consistency error $\mathcal{E}_f$.

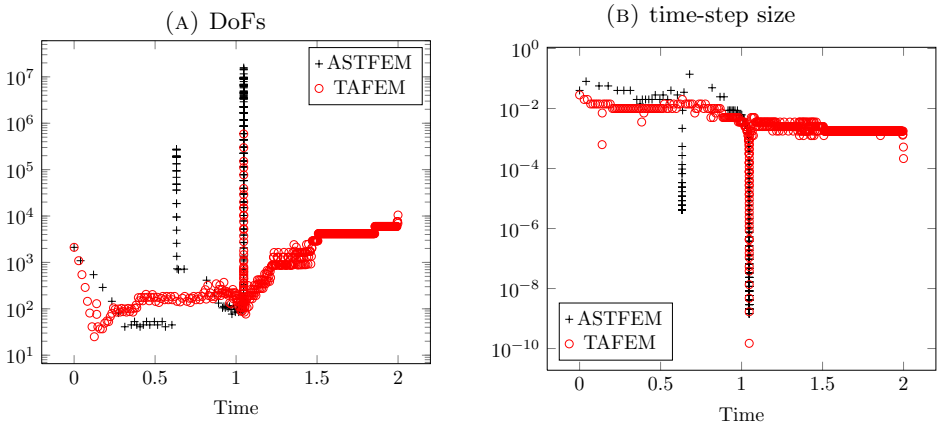

FIGURE 1. DoFs and time-step sizes for the singularity in time problem.

ASTFEM was killed after time-step 288 in which 14 163 460 DoFs are used as well as a time-step size of 1.46338e−9. As can be observed from Figure 1, ASTFEM massively refines in time and space. It was killed before reaching the singularity at $\bar{t} = \frac{\pi}{3}$, thereby accumulating the total number of 498 228 711 DoFs. The reason for this behaviour lies in the L^∞ marking. Indeed, Figure 2 shows that ASTFEM equally distributes the L^∞ indicators thereby leading to very small local errors, which cause the strong spatial refinement. Note that the minimal step-size τ_* in ASTFEM only applies when temporal refinement is performed due to the time indicator $\mathcal{E}_\tau$, i.e., time-step sizes below the threshold can τ_* be chosen when required by the consistency estimator $\mathcal{E}_f$, which is the case close to the singularity. Consequently, the behaviour of ASTFEM cannot essentially improved by a different choice of $\mathtt{TOL}_*$. In contrast, the local estimators TAFEM appears to be quite equally distributed. It uses slightly larger time-steps and by far less DoFs close to the singularity; compare with the table of Fig. 3. It completely outperforms ASTFEM and reaches the final time with a total of 2 947 080 DoFs in 618 time-steps.

6.2.2. *Jumping singularity.* Inspired by example 5.3 of [MNS00], we construct an experiment where the solution has a strong spatial singularity that changes its

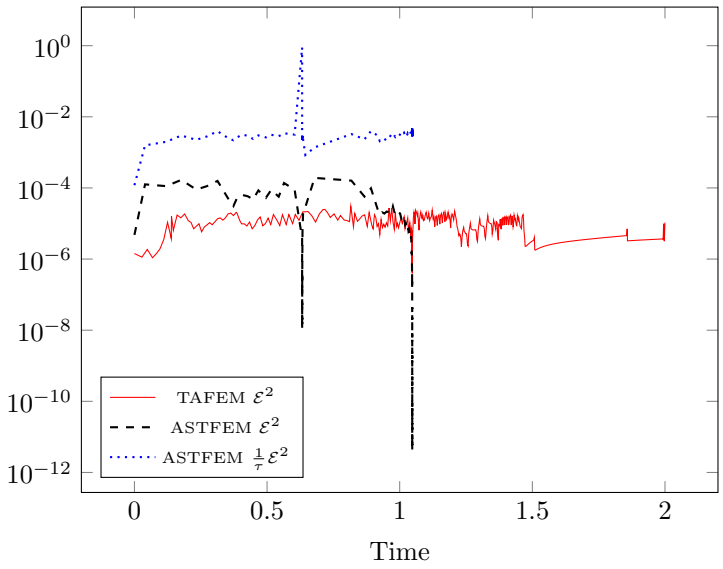

FIGURE 2. The local error estimators $\mathcal{E}_\tau^2+\mathcal{E}_\mathcal{G}^2+\mathcal{E}_c^2+\mathcal{E}_f^2$ for TAFEM and ASTFEM as well as the sum of local L^∞ indicators $\frac{1}{\tau}(\mathcal{E}_\tau^2+\mathcal{E}_\mathcal{G}^2+\mathcal{E}_c^2+\mathcal{E}_f^2)$ used by ASTFEM for the singularity in time problem.

time	time-step ASTFEM	DoFs ASTFEM	time-step TAFEM	DoFs TAFEM
1.0	0.00613614	97	0.00353598	193
1.02	0.00433893	85	0.00353601	112
1.03	0.0030681	97	0.00250034	109
1.04	0.00153406	97	0.00125018	109
1.042	0.00108475	97	0.00125018	125
1.044	0.00108475	97	0.000884012	132
1.045	0.000542376	157	0.000625091	128
1.046	0.000383519	193	0.000312546	242
1.047	3.3899e-05	713	7.81367e-05	448
1.0471	1.19852e-05	2073	3.90684e-05	635
1.0472	9.36409e-08	226082	1.7266e-06	3693
1.0473	*non*	*non*	3.90691e-05	622

FIGURE 3. Time-steps and DoFs of ASTFEM and TAFEM for the singularity in time problem.

position in time. In the domain $\Omega \times (0,4]$, with $\Omega = (0,3) \times (0,3)$, we define the elliptic operator $\mathcal{L}u = -\operatorname{div} \mathbf{A}\nabla u$, where

$$\mathbf{A}(t,x) = \begin{cases} a_1\mathbb{I} & \text{if } (x-x_i)(y-y_i) \geqslant 0 \\ a_2\mathbb{I} & \text{if } (x-x_i)(y-y_i) < 0 \end{cases}$$

with $a_1 = 161.4476387975881$, $a_2 = 1$, $i = \lceil t \rceil$, $(x_1,y_1) = (1,2)$, $(x_2,y_2) = (1,1)$, $(x_3,y_3) = (2,1)$, and $(x_4,y_4) = (2,2)$. This operator will 'move' the singularity through the points x_i. Let u be the function

$$u(x,t) = \sum_{i=1}^{4} s_i(t)\, r_i^\gamma\, \mu(\theta_i)$$

where

$$s_i(t) = \begin{cases} (t-(i-1))^2(t-i)^2 & \text{if } i-1 \leqslant t \leqslant i \\ 0 & \text{otherwise} \end{cases}$$

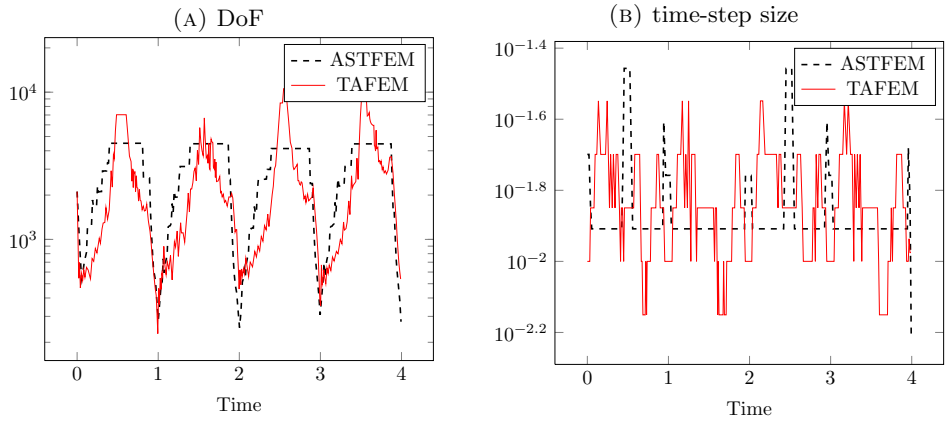

FIGURE 4. DoFs and time-step sizes for the jumping singularity problem.

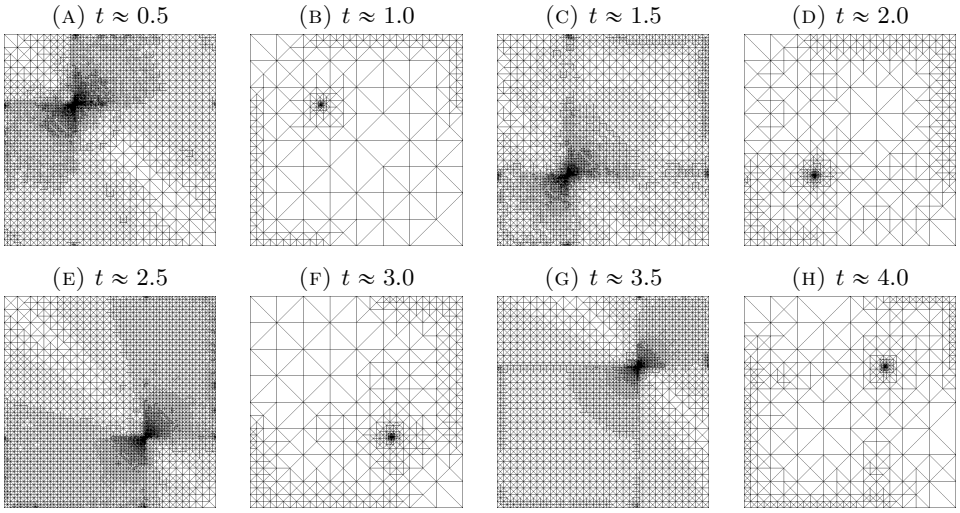

FIGURE 5. Adaptive grids for the jumping singularity problem.

and

$$\mu(\theta) = \begin{cases} \cos((\frac{\pi}{2} - \sigma)\gamma) \cdot \cos((\theta - \frac{\pi}{2} + \rho)\gamma) & \text{if } 0 \leqslant \theta < \frac{1}{2}\pi \\ \cos(\rho\gamma) \cdot \cos((\theta - \pi + \sigma)\gamma) & \text{if } \frac{1}{2}\pi \leqslant \theta < \pi \\ \cos(\sigma\gamma) \cdot \cos((\theta - \pi - \rho)\gamma) & \text{if } \pi \leqslant \theta < \frac{3}{2}\pi \\ \cos((\frac{\pi}{2} - \rho)\gamma) \cdot \cos((\theta - \frac{3\pi}{2} - \sigma)\gamma) & \text{if } \frac{3}{2}\pi \leqslant \theta < 2\pi \end{cases}$$

with $\gamma = 0.1$, $\rho = \frac{\pi}{4}$, $\sigma = -14.92256510455152$, $x - x_i = r_i \cos(\theta_i)$ and $y - y_i = r_i \sin(\theta_i)$. It is easy to check that u satisfies

$$\partial_t u(x,t) + \mathcal{L}u(x,t) = \sum_{i=1}^{4} r_i^\gamma \mu(\theta_i)\ \partial_t s_i(t)\ .$$

Based on the ideas presented in Remark 22 we compare TAFEM and ASTFEM with the same tolerance $\texttt{TOL} = 0.007$.

ASTFEM makes excessive use of the nonstandard exit, i.e., the time-step sizes equal minimal time-step size $\tau_* = 0.0123477$ for 276 of a total of 302 time-steps, and uses a total of 893771 Dofs. The $L^2 - H^1$-error is 0.0546689, the $L^2 - L^2$-error is 0.0355061 and the total computation time was 413.67 seconds.

The TAFEM uses a total of 786789 Dofs in 291 time-steps. The $L^2(0,4,H^1(\Omega))$-error is 0.0552438, the $L^2(0,4,L^2(\Omega))$-error is 0.034989 and the total computation time was 546.113 seconds (including `TOLFIND`). The adaptive meshes generated by TAFEM are displayed in Figure 5. We see that the spatial adaptivity captures the position of the singularity by local refinement and coarsens the region when the singularity has passed by. By having a look on Fig. 4 we see, that TAFEM makes more use of the spatial and temporal adaptivity and achieves a similar result with slightly less effort.

The advantages of TAFEM come fully into their own in the presence of singularities in time (see Section 6.2.1). For regular (in time) problems, TAFEM is expected to perform similar to ASTFEM up to the disadvantage that, at the beginning, the module `TOLFIND` needs several adaptive iterations over the time span, whereas the computation for the minimal time-step size in ASTFEM only iterates once over the time. This is reflected in the comparable computing times for the jumping singularity problem.

6.2.3. *Rough initial data.* We conclude with an example inspired on the numerical experiment 5.3.2 in [KMSS12] with homogeneous Dirichlet boundary conditions and homogeneous right-hand side $f \equiv 0$. As initial data we choose a checkerboard pattern over $\Omega = (0,1)^2$ where $u_0 \equiv -1$ on $\Omega_1 = (\frac{1}{3},\frac{2}{3}) \times \big((0,\frac{1}{3}) \cup (\frac{2}{3},1)\big) \cup \big((0,\frac{1}{3}) \cup (\frac{2}{3},1)\big) \times (\frac{1}{3},\frac{2}{3})$, $u_0 \equiv 1$ on $\Omega\backslash\Omega_1$ and $u_0 \equiv 0$ on $\partial\Omega$. Starting with an initial mesh with only 5 DoFs, the approximation of u_0 uses Lagrange interpolation and refines the mesh until $\|U_0 - u_0\|_\Omega^2 \leqslant \mathtt{TOL}_0^2 = 10^{-2}$ is fulfilled. Starting ASTFEM and TAFEM with a tolerance of $\mathtt{TOL} = 10^{-1}$ and running to the final time $T = 1$, we get the following results: ASTFEM needs 811 time-steps, a total sum of 436 199 377 DoFs, with an estimated total error of 0.0230905, and a total computation time of 81466.4 seconds. The ASTFEM makes use of the nonstandard exit for the first 270 time-steps, with minimal time-step size of $\tau_* = 7.77573\mathrm{e}{-7}$, the small size of the time-steps in the beginning is also accompanied by extreme spatial refinements contributing to the large total number of DoFs. This is due to the L^∞-strategy that aims in an equal distributing of the time-indicators $\frac{1}{\tau}\mathcal{E}_\tau^2$ rather then $\mathcal{E}_\tau^2$. In order to highlight this effect close to the initial time, we have used a log scale for the time in Figures 6 and 7. The TAFEM only needs 117 time-steps and a total of 3 762 503 DoFs resulting in an estimated total error of 0.039855. It is about 20 times faster with a total computation time of 3903.76 seconds (including `TOLFIND`). TAFEM refines the mesh initially and then almost steadily coarsens in time and space (see Figures 7 and 8 (E-H)). Figure 6 shows that the time indicators $\mathcal{E}_\tau^2$ are nearly equally distributed. Both algorithms reduce the spatial resolution once the singular behaviour of the solution is reduced; see Figures 7 and 8.

References

[AMN09] Georgios Akrivis, Charalambos Makridakis, and Ricardo H. Nochetto, *Optimal order a posteriori error estimates for a class of Runge-Kutta and Galerkin methods*, Numer. Math. **114** (2009), no. 1, 133–160.

[Bän91] E. Bänsch, *Local mesh refinement in 2 and 3 dimensions*, IMPACT Comput. Sci. Engrg. **3** (1991), 181–191.

[BBD+16] M. Blatt, A. Burchardy, A. Dedner, Ch. Engwer, J. Fahlle, B. Flemisch, C. Gersbacher, C. Gräser, F. Gruber, C. Grüninger, D. Kempf, R. Klöfkorn, T. Malkmus, S. Müthing, M. Nolte, M. Piatkowski, and O. Sander, *The Distributed and Unified Numerics Environment (DUNE), Version 2.4*, Archive of Numerical Software **100** (2016), no. 4, 13–29.

[BDD04] P. Binev, W. Dahmen, and R. A. DeVore, *Adaptive finite element methods with convergence rates*, Numer. Math **97** (2004), 219–268.

[BDDP02] P. Binev, W. Dahmen, R. DeVore, and P. Petrushev, *Approximation classes for adaptive methods*, Serdica Math. J. **28** (2002), no. 4, 391–416, Dedicated to the memory of Vassil Popov on the occasion of his 60th birthday.

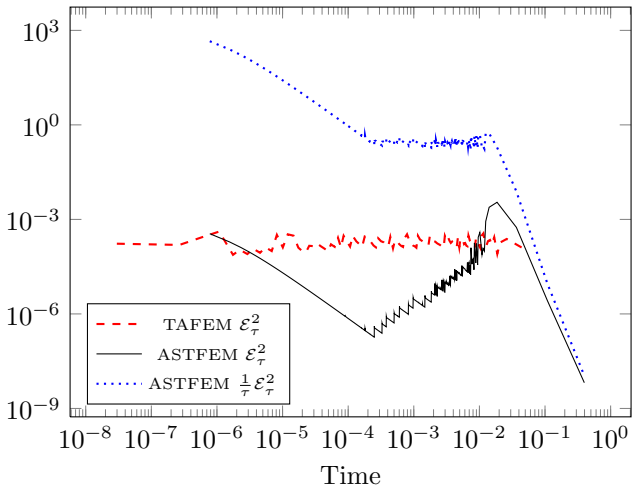

FIGURE 6. The local time indicator $\mathcal{E}_\tau^2$ for TAFEM and ASTFEM as well as the local L^∞ indicators $\frac{1}{\tau}\mathcal{E}_\tau^2$ used by ASTFEM for the rough initial data problem.

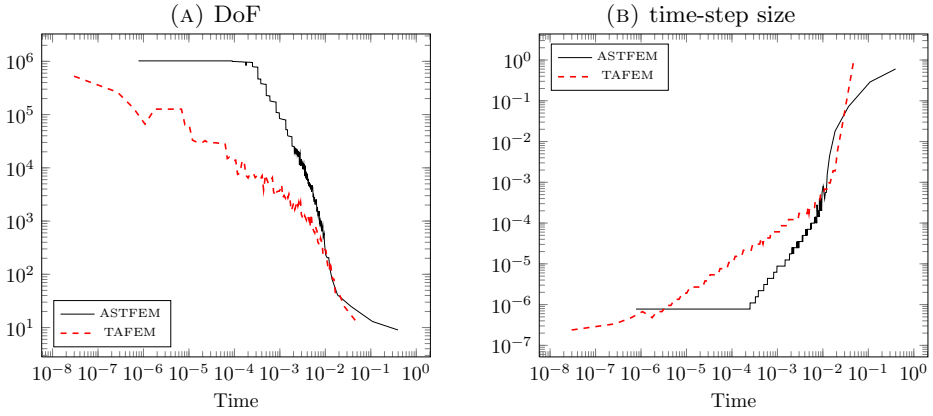

FIGURE 7. DoFs and time-step sizes for the rough initial data problem.

[CF04] Z. Chen and J. Feng, *An adaptive finite element algorithm with reliable and efficient error control for linear parabolic problems*, Math. Comp. **73** (2004), 1167–1193.

[CKNS08] J. M. Cascon, C. Kreuzer, R. H. Nochetto, and K. G. Siebert, *Quasi-optimal convergence rate for an adaptive finite element method*, SIAM J. Numer. Anal. **46** (2008), no. 5, 2524–2550.

[DK08] L. Diening and C. Kreuzer, *Convergence of an adaptive finite element method for the p-Laplacian equation*, SIAM J. Numer. Anal. **46** (2008), no. 2, 614–638.

[DKS16] L. Diening, C. Kreuzer, and R. Stevenson, *Instance Optimality of the Adaptive Maximum Strategy*, Found. Comput. Math. **16** (2016), no. 1, 33–68.

[Dör96] W. Dörfler, *A convergent adaptive algorithm for Poisson's equation*, SIAM J. Numer. Anal. **33** (1996), no. 3, 1106–1124.

[EJ91] K. Eriksson and C. Johnson, *Adaptive finite element methods for parabolic problems I: A linear model problem*, SIAM J. Numer. Anal. **28** (1991), 43–77.

[Eva10] L. C. Evans, *Partial differential equations*, second ed., Graduate Studies in Mathematics, vol. 19, American Mathematical Society, Providence, RI, 2010.

[ESV] A. Ern, I. Smears, and M. Vohralík, *Guaranteed, locally space-time efficient, and polynomial-degree robust a posteriori error estimates for high-order discretizations of parabolic problems*, submitted.

[GM14] F. D. Gaspoz and P. Morin, *Approximation classes for adaptive higher order finite element approximation*, Math. Comp. **83** (2014), no. 289, 2127–2160.

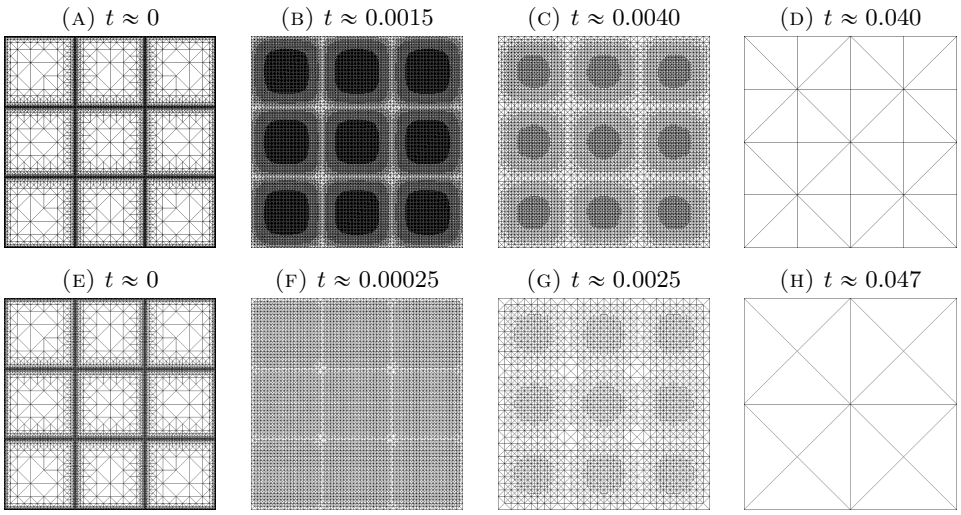

FIGURE 8. Adapted meshes generated with ASTFEM (A-D) and TAFEM (E-H) for the rough initial data problem.

[GT01] D. Gilbarg and N. S. Trudinger, *Elliptic partial differential equations of second order*, Classics in Mathematics, Springer-Verlag, Berlin, 2001, Reprint of the 1998 edition.

[KMSS12] C. Kreuzer, C. A. Möller, A. Schmidt, and K. G. Siebert, *Design and convergence analysis for an adaptive discretization of the heat equation*, IMA J. Numer. Anal. **32** (2012), no. 4, 1375–1403.

[Kos94] I. Kossaczký, *A recursive approach to local mesh refinement in two and three dimensions*, J. Comput. Appl. Math. **55** (1994), 275–288.

[KS11] C. Kreuzer and K. G. Siebert, *Decay rates of adaptive finite elements with Dörfler marking*, Numer. Math. **117** (2011), no. 4, 679–716.

[LM06] O. Lakkis and C. Makridakis, *Elliptic reconstruction and a posteriori error estimates for fully discrete linear parabolic problems*, Math. Comp. **75** (2006), no. 256, 1627–1658.

[Mau95] J. M. Maubach, *Local bisection refinement for n-simplicial grids generated by reflection*, SIAM J. Sci. Comput. **16** (1995), no. 1, 210–227.

[MN03] C. Makridakis and R. H. Nochetto, *Elliptic reconstruction and a posteriori error estimates for parabolic problems*, SIAM J. Numer. Anal. **41** (2003), no. 4, 1585–1594.

[MN05] K. Mekchay and R. H. Nochetto, *Convergence of adaptive finite element methods for general second order linear elliptic PDEs*, SIAM J. Numer. Anal. **43** (2005), no. 5, 1803–1827 (electronic).

[MNS00] P. Morin, R. H. Nochetto, and K. G. Siebert, *Data oscillation and convergence of adaptive FEM*, SIAM J. Numer. Anal. **38** (2000), no. 2, 466–488 (electronic).

[MNS02] ———, *Convergence of adaptive finite element methods*, SIAM Rev. **44** (2002), no. 4, 631–658 (electronic) (2003), Revised reprint of "Data oscillation and convergence of adaptive FEM" [SIAM J. Numer. Anal. **3**8 (2000), no. 2, 466–488 (electronic)].

[MSV08] P. Morin, K. G. Siebert, and A. Veeser, *A basic convergence result for conforming adaptive finite elements*, Math. Models Methods Appl. Sci. **18** (2008), no. 5, 707–737.

[NSV09] R. H. Nochetto, K. G. Siebert, and A. Veeser, *Theory of adaptive finite element methods: an introduction*, Multiscale, nonlinear and adaptive approximation, Springer, Berlin, 2009, pp. 409–542.

[Pic98] M. Picasso, *Adaptive finite elements for a linear parabolic problem*, Comput. Methods Appl. Mech. Engrg. **167** (1998), no. 3-4, 223–237.

[Sie11] K. G. Siebert, *A convergence proof for adaptive finite elements without lower bound.*, IMA J. Numer. Anal. **31** (2011), no. 3, 947–970 (English).

[Sme15] I. Smears, *Robust and efficient preconditioners for the discontinuous galerkin time-stepping method*, Technical report 1894, University of Oxford, 2015.

[SS05] A. Schmidt and K. G. Siebert, *Design of adaptive finite element software*, Lecture Notes in Computational Science and Engineering, vol. 42, Springer-Verlag, Berlin, 2005, The finite element toolbox ALBERTA, With 1 CD-ROM (Unix/Linux).

[SS09] C. Schwab and R. Stevenson, *Space-time adaptive wavelet methods for parabolic evolution problems*, Math. Comp. **78** (2009), no. 267, 1293–1318.

[Ste07] R. Stevenson, *Optimality of a standard adaptive finite element method*, Found. Comput. Math. **7** (2007), no. 2, 245–269.

[Tho06] V. Thomée, *Galerkin finite element methods for parabolic problems*, second ed., Springer Series in Computational Mathematics, vol. 25, Springer-Verlag, Berlin, 2006.

[Tra97] C. T. Traxler, *An algorithm for adaptive mesh refinement in n dimensions*, Computing **59** (1997), 115–137.

[TV16] F. Tantardini and A. Veeser, *Quasi-optimality constants for parabolic galerkin approximation in space*, Proceedings of the 10th European Conference on Numerical Mathematics and Advanced Applications held at the Middle East Technical University, Ankara, Turkey, September 14–18, 2015, To appear in Lecture Notes in Computational Science and Engineering, Springer, Heidelberg, 2016.

[Ver03] R. Verfürth, *A posteriori error estimates for finite element discretizations of the heat equation*, Calcolo **40** (2003), no. 3, 195–212.

[Ver13] ———, *A posteriori error estimation techniques for finite element methods*, Numerical Mathematics and Scientific Computation, Oxford University Press, Oxford, 2013.

Fernando D. Gaspoz, Institut für Angewandte Analysis und Numerische Simulation, Fachbereich Mathematik, Universität Stuttgart, Pfaffenwaldring 57, D-70569 Stuttgart, Germany

URL: www.ians.uni-stuttgart.de/nmh/

E-mail address: fernando.gaspoz@ians.uni-stuttgart.de

Christian Kreuzer, Fakultät für Mathematik, Ruhr-Universität Bochum, Universitätstrasse 150, D-44801 Bochum, Germany

URL: http://www.ruhr-uni-bochum.de/ffm/Lehrstuehle/Kreuzer/index.html

E-mail address: christan.kreuzer@rub.de

Kunibert G. Siebert, Institut für Angewandte Analysis und Numerische Simulation, Fachbereich Mathematik, Universität Stuttgart, Pfaffenwaldring 57, D-70569 Stuttgart, Germany

URL: www.ians.uni-stuttgart.de/nmh/

E-mail address: kg.siebert@ians.uni-stuttgart.de

Daniel A. Ziegler, Institut für Angewandte und Numerische Mathematik, Karlsruher Institut für Technologie, Englerstrsse 2, D-76131 Karlsruhe, Germany

URL: http://www.math.kit.edu/~daniel.ziegler

E-mail address: daniel.ziegler@kit.edu